Aalto University
School of Science

Juuso Lindgren

Energy strategies for electric mobility in urban areas

Master's thesis submitted in partial fulfillment of the requirements for the degree of Master of Science in Technology in the Degree Programme in Engineering Physics and Mathematics.

Espoo, 10.01.2012

Supervisor: Professor Peter Lund

Instructor: M. Sc. Rami Niemi

Aalto University School of Science	ABSTRACT OF THE MASTER'S THESIS

Author: Juuso Lindgren

Title: Energy strategies for electric mobility in urban areas

Title in Finnish: Sähköajoneuvojen latausstrategioista kaupunkiympäristössä

Degree Programme: Degree Programme in Engineering Physics and Mathematics

Major subject: Engineering Physics	Minor subject: Computational Science and Engineering

Chair (code): Tfy-56

Supervisor: Prof. Peter Lund	Instructor: M.Sc. Rami Niemi

Abstract:

Due to global environmental concerns, plug-in hybrid electric vehicles (PHEVs) are expected to become more prevalent. In order to avoid overloading the power supply system and to use PHEV recharging to reduce power fluctuations, smart charging strategies could be very useful.

This thesis introduces a method for allocating available power to the connected PHEVs through a charging function. To obtain insight on the problem of power allocation, the form and parameters of the charging function were modified and the effect on the electric kilometers (objective function to be maximized) was checked. All results were obtained in a simulated environment, using Helsinki as a case.

The results indicate that it is usually a good strategy to allocate more charging power for vehicles that have low state of charge (SOC) and low battery capacity.

Obtaining an accurate prediction for the amount of time a PHEV will stay at its current location provides more electric kilometers than an accurate prediction for the amount of kilometers the PHEV will travel before reconnecting with the grid. It is possible to safeguard against inaccurate predictions by using a linear combination of the prediction and the observed average.

When there is a sufficient correlation between travelled distance and battery capacity, the effectiveness of our strategies diminishes, rendering them almost redundant. The effectiveness of any strategy is linked to the battery capacity. With too low and too high capacities, the strategies are redundant.

This thesis also introduces a method for generating nearly arbitrary charging load profiles for night-time home recharging, the weighted random recharging (WRR). It was shown that with traffic electrification of 39 % and under certain simplifying assumptions, the yearly standard deviation of power consumption could be reduced by 6.3 % while reducing the daily standard deviation by 61 % on average.

Date: 10.1.2012	Language: English	Number of pages: 64

Keywords: PHEV, plug-in hybrid, vehicle, recharging

Aalto-yliopisto Perustieteiden korkeakoulu	DIPLOMITYÖN TIIVISTELMÄ
Tekijä: Juuso Lindgren	
Työn nimi: Sähköajoneuvojen latausstrategioista kaupunkiympäristössä	
Title in English: Energy strategies for electric mobility in urban areas	
Tutkinto-ohjelma: Teknillisen fysiikan ja matematiikan tutkinto-ohjelma	
Pääaine: Teknillinen fysiikka	Sivuaine: Laskennallinen tiede ja tekniikka
Opetusyksikön (ent. professuuri) koodi: Tfy-56	
Työn valvoja: Prof. Peter Lund	Työn ohjaaja(t): M.Sc. Rami Niemi

Tiivistelmä:

Maailmanlaajuisten ympäristöongelmien uhan vuoksi on odotettavissa, että plug-in hybridisähköajoneuvojen (PHEV) määrä tulee lisääntymään. Välttääksemme sähköjärjestelmämme ylikuormittamisen ja jopa hyötyäksemme sähköajoneuvojen latauskuormasta pienentämällä tehonkulutuksen vaihtelua älykkäät latausstrategiat voivat osoittautua hyödyllisiksi.

Tämä diplomityö esittelee latausfunktion, menetelmän tehon jakamiselle sähköverkkoon kytketyille autoille. Yritimme ymmärtää tehon jakamisen ongelmaa kokeilemalla erilaisia muotoja tälle funktiolle ja selvittämällä, miten ajettujen sähkökilometrien määrä, maksimoitavan kohdefunktiomme arvo, muuttui. Kaikki tuloksemme saavutettiin simuloidussa ympäristössä Helsinkiä edustavassa noodiverkostossa.

Tuloksemme viittaavat siihen, että on tavallisesti hyvä strategia antaa enemmän lataustehoa niille ajoneuvoille, joiden normalisoitu lataustaso (SOC) ja kapasiteetti ovat matalia.

Tarkan ennusteen saaminen sille ajalle, minkä ajoneuvo viettää nykyisessä sijainnissaan tuottaa enemmän sähkökilometrejä kuin tarkka ennuste sille matkalle, minkä ajoneuvo kulkee ennen liittymistään takaisin sähköverkkoon. Huonoja ennusteita vastaan voidaan suojautua käyttämällä ennusteen ja havaitun keskiarvon yhdistelmää.

Kun kuljetun matkan ja akkukapasiteetin välillä on riittävä korrelaatio, käyttämiemme strategioiden vaikutus pieneni tehden niistä lähes tarpeettomia. Minkä tahansa strategian vaikutus riippuu akkukapasiteetista. Liian pienillä ja liian suurilla kapasiteeteilla strategiat ovat tarpeettomia.

Tämä diplomityö esittelee myös menetelmän lähes mielivaltaisten latauskuormaprofiilien muodostamiselle, painotetun satunnaislatauksen (WRR). Näytämme, että liikenteen sähköistämisprosentin ollessa 39 ja tiettyjen yksinkertaistavien oletusten voimassaollessa voidaan vuosittaista sähkönkulutuksen keskihajontaa pienentää 6.3 % päivittäisen keskihajonnan pienentyessä keskimäärin 61 %.

Päivämäärä: 10.1.2012	Kieli: englanti	Sivumäärä: 64
Avainsanat: PHEV, plug-in hybridi, ajoneuvo, lataaminen		

Acknowledgements

This study is a part of the SIMBe project that was funded by the Finnish Funding Agency for Technology and Innovation (TEKES). The financial support is greatly appreciated.

I would like to thank M.Sc. Rami Niemi, B.Sc. Jani Mikkola and prof. Peter Lund from the New Energy Technologies research group in the Aalto University School of Science for their advice and support. I would also like to thank my family and friends for their continuous care and support over the years.

The simulation model has been developed using MATLAB® by MathWorks® (www.mathworks.com). Figures were created using MATLAB®, LibreOffice® by The Document Foundation® (www.libreoffice.org) and Inkscape 0.47 (www.inkscape.org). This document has been created in LaTeX using Texmaker 3.1 (www.xm1math.net/texmaker).

Contents

Nomenclature

c	Electricity consumption of a PHEV (kWh/km)
d_{ij}	Distance between nodes i and j (km)
dt	Length of the timestep (s)
e_i	Energy allocated to car i (kWh)
f_i	Fed-up factor of car i
m	Recharge time (min)
p	Power factor (kW), electrification percentage
r	Random number
s_{ij}	Score of node i relative to node j (km^{-1})
t	Time (s), timestep
t_{mid}	Recharging interval midpoint
t_{PP}	Peak position
w	Preference of prediction versus observed average
x	Normalized SOC
y	Capacity (kWh)
$\hat{y}$	The largest capacity (kWh)
z	Charging function
A_i	Attraction function of node i
D	Prediction for next free distance (km), energy deficit (kWh)
D_0	Exactly known next free distance (km)
E	Energy (kWh)
E_i	Available energy at node i (kWh)
$\check{E}$	Required energy (kWh)
F_i	Fed-up function of node i
N	Number of PHEVs
N_i	Amount of inhabitants at node i
P_i	Total recharging power at node i (kW)
P	Maximum charging power supported by battery (kW)
T	Prediction for stationary time
T_0	Exactly known stationary time
W	Weight vector
W_i	Weight of car i

α	Weight of SOC, weight of energy, weight of SOC deficit
β	Weight of capacity, weight of required energy
γ	Weight of stationary time
δ	Error in prediction
ϵ_D	Scaled error in the prediction for next free distance
ϵ_T	Scaled error in the prediction for stationary time
η	Weight of capacity
λ	Weight of SOC
σ_D	Scaling constant for next free distance prediction error
σ_{P}	Scaling constant
σ_T	Scaling constant for stationary time prediction error

Abbreviations

DCC Distance-capacity correlation. If DCC is included, cars that travel greater distances have bigger battery capacity. See section 5.1.4.

EDS *Each-day-separately*, see section 6.2.1.

FWHM Full width at half maximum.

ICE Internal combustion engine.

NSCI Null-strategy capacity increase. See *null-strategy capacity*.

SOC State of charge of a battery i.e. the amount of electric energy that is stored in a battery. This can also mean normalized SOC, where number 1 refers to a fully recharged battery and 0 to a fully discharged battery. In this thesis, we mainly use the term SOC to refer to the normalized SOC [1].

WRR See *weighted random recharging*.

WY1 *Whole-year-at-once*, see section 6.2.1.

Terminology

Throughout this thesis, we will use the terms *car*, *vehicle* and PHEV interchangeably.

bandwidth The magnitude of the power that can be used for recharging a single car or a group of cars.

big factor When two different battery capacities are used, this is the fraction of the cars that have the larger battery capacity.

free distance The distance a car travels between two different charging sessions.

high-priority car A car that should be given more *bandwidth* in an intelligent charging strategy.

low-priority car A car that should be given less *bandwidth* in an intelligent charging strategy.

null-strategy The charging strategy with no intelligence. This strategy attempts to allocate the available bandwidth to all connected cars equally.

null-strategy capacity See section 3.4.2.

smart charging Intelligent allocating of charging *bandwidth* for cars or groups of cars.

[1] If the battery has an operating range, the normalization is assumed to be relative to the operating range so that a battery that has energy 1 kWh stored, but does not allow discharging below this level, is considered to have SOC of 0.

stationary time The remaining time the car will stay at its current location.

weighted random recharging See section 6.1.

working day A day that is not Saturday or Sunday.

If some amount of electric energy is not used to move a vehicle during a simulation, and it could have been used to move another vehicle using some other charging strategy, it is called *wasted*.

When the charging power of some car or a group of cars A is limited due to some other car or a group of cars B having more charging power, for example due to favoring in smart charging, we say that B is *hogging the bandwidth* with respect to A.

1 Introduction

One of the greatest current challenges faced by mankind is the struggle against anthropogenic climate change, the worldwide increase in average temperature that threatens to cause irreversible and chaotic changes to the environment.

In order to counteract global warming, it is widely believed that severe reductions in greenhouse gas emissions are required. A major factor in these emissions is the transport sector, which is responsible for around 25 % of worldwide CO_2 emissions, 75 % of this being attributable to cars and trucks [1]. With countries around the world signing environmental treaties and the natural oil reserves running dry, it seems that there is need for a revolution in the powertrain. One such revolution is offered by the electric vehicle, which enables utilizing alternative energy sources for providing the power needed for transportation.

The path to electrification of transportation is not free of obstacles. A major impediment is the relatively long recharge time of the battery due to limiting factors in the battery chemistry and power supply. Another drawback is the low energy density of a PHEV battery, which is two orders of magnitude lower than that of gasoline [2][3]. This, in turn limits either the range of the cars due to the capacity being insufficient or the amount of passengers on the car due to having too much space occupied by batteries[2].

An intermediate stage could be necessary. The plug-in hybrid electric vehicle, PHEV, is a vehicle that combines the benefits of the electric vehicle and the long range and rapid refueling time of the ICE vehicle. Unlike the ordinary hybrid vehicle, the plug-in hybrid supports recharging from the electric grid, which enables driving completely carbon-free, assuming carbon-free electricity production.

The possible reductions in emissions is not the only benefit of a PHEV, for the PHEV can also be used to provide positive and negative load to the grid. For example, it is possible to use the recharging of PHEVs to fill the night slump in the electric power consumption. This is beneficial, because with a more uniform power consumption, there is no need to shut down power plants or operate them outside their high-efficiency range. By providing positive load, PHEVs can also be used to level power production spikes caused by wind or solar power plants. Providing negative load i.e. transferring power from the battery to the grid, can be used to provide back-up power and to level negative production spikes.

Having a large number of PHEVs interacting with the electric grid provides its own challenges. It is highly unlikely that millions of PHEVs will be allowed to recharge whenever they wish as this may cause massive load spikes at points where the load is already high as it is, for example, when returning home from work. There is need for intelligent charging strategies that tell us when and how they are allowed to recharge.

The goal of this thesis is to study smart charging strategies using a simulation model for the movement and charging for PHEVs. We will search for optimal ways to recharge the connected vehicles when the electric grid is

[2]In the case of a fully electric car, the *effective* energy density may be better than that of an internal combustion engine (ICE) car. For hybrids, however, this is not the case, because they need to accommodate both an ICE and an electric engine. [4]

under heavy load, limiting the available power for recharging. If the power is limited, it may be that there is not enough energy to fully recharge all connected vehicles. Instead of allocating the available power equally, we could favor some vehicles over others. This method could be used to increase the total amount of kilometers driven using electricity, our objective function. The main approach for adding intelligence to the recharging process is the charging function, which tells how the available power should be divided between the connected cars.

We also study a way of decreasing the fluctuation in the power consumption by concentrating the recharging load to the night-time consumption slump. For this, a method for generating almost arbitrary charging load profiles during night-time home recharging is proposed.

2 Background

Vehicle-to-grid, or V2G, is used to describe the situation where plug-in electric vehicles (PEV) communicate with the electric grid in order to provide demand response services. An example of such a service is the throttling of charging power at times of high base consumption and timing the charging to happen during the night, when the base consumption is high. It has been calculated that grid overloading can be significantly reduced by smart charging while satisfying the individual vehicle owner's requirements [5]. Also, by using smart charging, the grid is able to support a larger share of electric vehicles before the system's technical restrictions are violated [6].

Kempton et al. (2005) have studied the feasibility of using PEVs to provide V2G services. They have suggested strategies and business models and the steps that are necessary for the implementation of V2G [7][8]. There has been a practical demonstration about the feasibility of using a PHEV to provide ancillary services such as frequency regulation. The PHEV used in the demonstration was custom-built with battery capacity of 35 kWh and with power electronics designed for both driving and to allow for high-power exchange with the grid. They concluded that electric vehicles are capable of providing ancillary services [9].

Being capable of providing positive and negative load, V2G can be used to balance intermittent power production. The applicability of V2G to renewable power production balancing in the case of wind power has been studied in [10][11][8]. The conclusions were that PEVs can be used as a means to regulate wind power.

Automotive manufacturers have also taken interest on V2G. Nissan, Mitsubishi and Toyota are developing new devices for the Japanese market that enable V2G for consumers [12]. Nissan's Power Control System allows the Nissan Leaf EV to feed 6 kW of electric power to home, which is sufficient to satisfy the needs of an average Japanese residence for two days. This system is expected to commercialize by October 2012 [13]. Mitsubishi i-MiEV and Toyota Estima hybrid van were used after the March 2011 natural disaster to provide emergency electric power in affected communities. Mitsubishi is hoping to put a V2G system to its coming crossover PHEV, concept name PX-MiEV. Toyota is expected to add this functionality to the 2012 Prius PHEV [12].

As for smart recharging, Su and Chow (2011) have studied an algorithm for optimally managing a large number (500) of PHEVs charging at a municipal charging station. The objective function was the average SOC for all vehicles at the next timestep. They considered energy price, charging time and current SOC [14].

Su and Chow (2011) have also proposed two smart charging scenarios. In the first scenario, the energy required to fully recharge the battery is evenly distributed over the period of expected parking time. In the second scenario, the current price of electricity was employed to determine the most cost-effective charging scenario on a per vehicle basis. They concluded that these strategies can improve stability and reliability of the power grid [15].

There have been studies with the optimization objective of minimizing the overall cost of charging the EV fleet. See e.g. [5][16]. In [16], battery

health degradation was also considered. Mets et al. (2010) [17] aimed to minimize the peak load and flatten the overall load profile. Clement et al. (2009) [18] optimized the charging by minimizing power losses.

Galus et al. (2011) [19] used a highly sophisticated agent-based transportation simulation to obtain temporal and spatial information of PHEV behavior, such as connection times and energy demands. These inputs were then used in power systems simulations. The objective was maximizing the sum of agent-specific utility functions, with power constraints. The utility functions in turn model the utility gained from increased SOC, while accounting for the price of gasoline and electricity. 15-minute timesteps were used in the study.

In contrast, our traffic model and objective functions are relatively simple. Instead of using an agent-based utility approach with explicit energy price considerations, we use a pooled utility objective, where the grid and power supply limitations and the effect of energy price are both combined to node-specific power limitations. To our knowledge, there are no other works which have used an analytical function for the problem of optimal power allocation. We are not aware of other studies that have used electric kilometers as the objective function and ones that have used imperfect predictions for e.g. parking time and discussed how the increase of error in the prediction relates to utility loss.

Algorithms for filling the night-slump have been proposed before. In a study conducted by Gan et al. (2010) [20], the cars choose their own charging profiles based on control signals (e.g. prices) sent by the utility. In this thesis, the charging process is centralized in the sense that the utility provides the midpoint for the charging interval. Our approach is arguably simpler, but relies on randomness, which may render it impractical with small numbers of vehicles.

3 Methods

The effects of different charging strategies are studied using a PHEV movement and charging simulation model developed in our research group. The main assumptions behind the simulation are documented in this section. The mechanics of the model itself along with additional assumptions are described in section 4. These assumptions, along with the ones introduced in section 4, will be used throughout this thesis unless otherwise mentioned.

3.1 Cars, battery, recharging and traffic

Each car in the simulation is a PHEV, so it is equipped with both a battery and a fuel tank. It is assumed that each car consumes 200 watt-hours per kilometer and travels with the speed 60 km/h. After (and *only* after) the car's battery runs out, it begins depleting its fuel tank. Fuel consumption is assumed equal for all cars. It is also assumed that the cars are fuelled sufficiently, so that they cannot run out of gas during the simulation. Stopping for refueling is not modelled.

Several different battery capacities will be used in the simulations performed in this thesis. A linear model is assumed for the charging of the battery. A study conducted by Sundström and Binding (2010) shows that the error due to this approximation is small [5].

For simplicity, it is assumed that all vehicles will attempt to recharge whenever they are stationed at a node that has charging sockets. It is also assumed that there are enough charging sockets to allow all parked cars to connect to the grid. All vehicles are assumed to have full SOC at the start of the simulation due to the considerations in 4.5.4.

For simplicity, traffic congestion is not modelled in any way. In this simulation, a travelling car does not move on the roads connecting the nodes, but occupies a special node called *transit space*, remains there for the time corresponding to the time it would take to travel physically using the road network, and then emerges at its destination.

3.2 Time period

A working day from 0:00 to 23:55 is simulated using five-minute timesteps. Working days were chosen to be simulated because the main mechanics of working days are well understood and almost unchanging. There is the commute from home to work, the commute from work to home and for some people, additional trips to shops and hobbies. The days of rest are less systematic in comparison. Due to the working days being in the majority and their unchanging nature, only 1-2 consecutive days are simulated, which saves computation time. Because the seasonal differences to the working day mechanics are intuitively negligible, no assumptions are made about the time of year.

3.3 Cross-battery energy transfer

It is assumed that there is no direct energy transfer between any two different cars. This means that no car may lower its energy level to increase

another's. This assumption has been made primarily for simplicity, but there are also other reasons for not wanting to use this charging process.

One reason for disallowing cross-battery energy transfer is that energy traffic causes wear to the participating battery [21]. If there is cross-battery energy transfer, the total energy traffic is expected to increase, as those batteries that transfer energy to other batteries may need to be recharged later on. The utility gained using cross-battery energy transfer would thus be offset by the need to replace the batteries earlier.

Cross-battery energy transfer also increases heat losses. Suppose that the node has E amount of energy to dispense to a single car and that the electrical-chemical energy conversion efficiency for all cars is $\epsilon < 1$ (in both directions). When recharging this car, the node loses E energy, but the car gains only ϵE energy. If a fraction x of this energy is used to recharge another car, the other car receives only $x\epsilon^3 E$, because there are two conversions (chemical-to-electrical and electrical-to-chemical) on the way from the first car to the other. Thus, when transmitting energy from the node to a car to another car, the total energy gained by the second car is proportional to ϵ^3.

3.4 Measuring the quality of a strategy

In order to rank competing strategies, a simple way of condensing the massive amount of data produced in the simulation is required, preferably one that produces a single scalar value. Two different gauges for measuring the quality of a strategy are used in this thesis: electric kilometers and null-strategy capacity increase (NSCI).

3.4.1 Electric kilometers

The amount of electric kilometers measures both the electrification of traffic and the *possible* reduction in carbon dioxide emissions. The notion that a kilometer has been driven using electricity instead of gasoline does *not* imply that the carbon emissions have reduced. In fact, if the electricity is produced using fossil fuels, the carbon emissions may *increase* [22]. By focusing on the electric kilometers and not carbon emissions reduction, there is no need to make any assumptions on the way the energy is produced.

The problem with this gauge is that the electric kilometers are not always "equal". An electric kilometer driven by a car that has a high fuel consumption reduces carbon emissions more than a kilometer driven by a car that has a low fuel consumption, assuming carbon-free electricity production. To negate this, we assumed that all vehicles have the same fuel consumption.

3.4.2 Null-strategy capacity

If there is only one available battery capacity for the simulated cars, it is possible to associate the electric kilometers with a certain capacity. Assuming the same power limitations, for every electric kilometer gain e there exists exactly one capacity augmentation that could increase the electric kilometers by the same amount e when no charging strategy is used, and

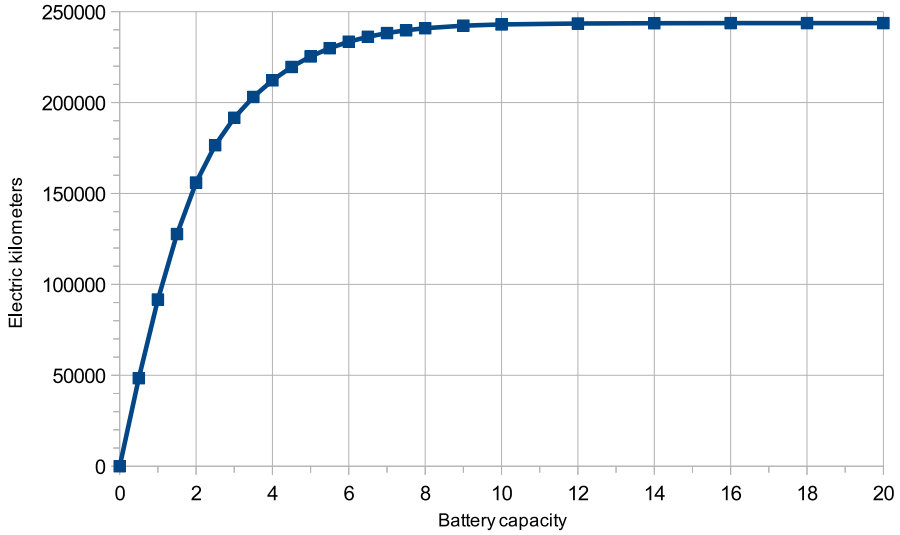

Figure 1: Electric kilometers as a function of battery capacity using the null-strategy. This curve is used in the conversion from electric kilometers to battery capacity. A cubic spline (not shown) is used to interpolate between the measured points (blue squares). Maximum power supported by a socket is 7.4 kW, home power factor is infinite, work power factor is 0.1 kW. See section 4.5 for the definition of the power factor.

vice versa. This increase in capacity is called the *null-strategy capacity increase*, or NSCI.

"No charging strategy", or *null-strategy*, refers to the case where the charging function z is constant, see section 3.4. With this strategy, the algorithm attempts to distribute the available power evenly to the connected cars. The curve used in this conversion is shown in Figure 1.

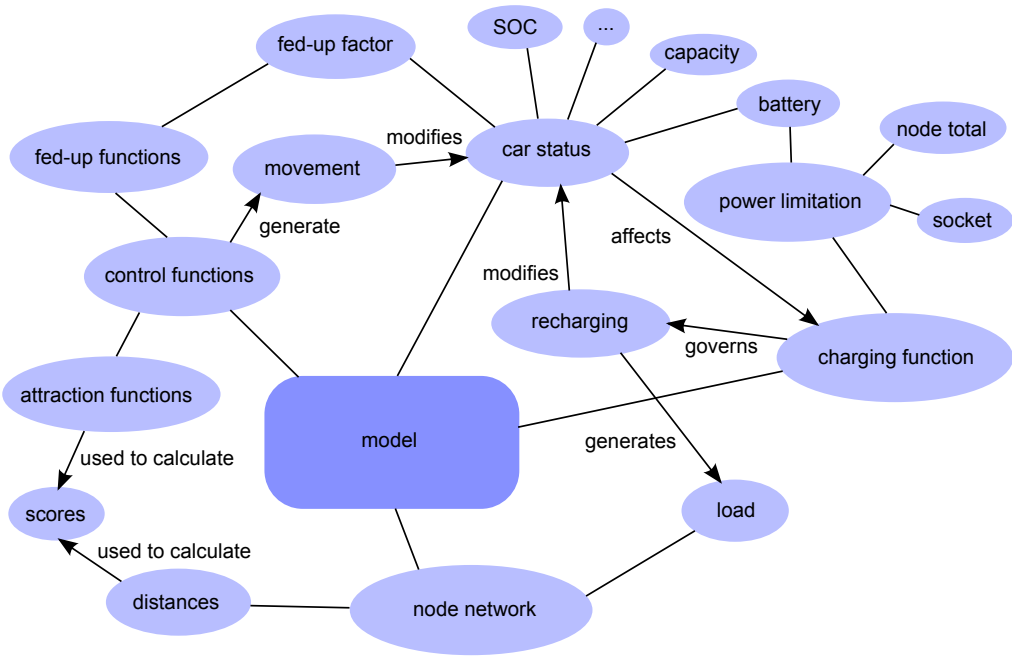

Figure 2: Schematic of the model.

4 Simulation model

The MATLAB®-based model used in this thesis simulates the movement and charging of PHEVs in a node network. The movement of the vehicles is based on *control functions*, while the charging is governed by the *charging function*. A schematic of the model is shown in Figure 2.

4.1 Control functions

There are two types of control functions: *attraction functions* and *fed-up functions*. Both are one-dimensional functions of time. The attraction functions are used to attract the cars to specific nodes at specific times and the fed-up functions are used to determine when the car will leave its current node.

4.1.1 Attraction functions

Attraction functions $A(t) \geq 0$ are node-specific functions of simulated time t that are used to decide the car's next destination. The attraction of node i at time t is denoted by $A_i(t)$. This value is divided by the car's distance to the node d_{ij}, where j is the node the car is currently occupying, to obtain a *score* s_{ij}:

$$s_{ij} := \frac{A_i(t)}{d_{ij}} \tag{1}$$

Because $d_{jj} = 0$ by definition, the score for the node the car is occupying is manually overridden to zero. Without this correction, the cars would never leave their current node. These scores are calculated for all possible candidates i.e. all nodes with nonzero attraction. The sum of these scores is then scaled linearly to 1 (*normalized*) and a uniformly distributed random number between 0 and 1 is used to select the destination[3]. The probability of being chosen as the next destination is proportional to the normalized score.

4.1.2 Fed-up functions and fed-up factors

Fed-up factor $f \in [0,1]$ is a car-specific value which determines how soon the car will leave its current node. A smaller fed-up factor implies that the car will leave its node earlier. f is picked from a suitable distribution before the simulation starts and each time the car leaves its current node. In this thesis, f, is generated using the method explained in A.1.

Fed-up functions $F_i(\tilde{t}) \in [0,1]$ are node-specific functions of occupation time $\tilde{t}$ i.e. the time the car has spent at its current location. Because of this, each car occupying the same node reads its own value of the fed-up function. The value of the fed-up function for car c that has been stationed at node i for $\tilde{t}_c$ timesteps, the current *fed-up value* of car c, is denoted by $F_i(\tilde{t}_c)$. When this value is greater than or equal to the fed-up factor $f_c \in [0,1]$ i.e. when

$$F_i(\tilde{t}_c) \geq f_c \tag{2}$$

the car begins travelling to the next destination according to the attraction functions. If there are no valid destination candidates (nodes with nonzero attraction), the car will stay at the current node until there is a valid destination, at which point the car will begin travel immediately. It should be noted that a sensible fed-up function should be monotonously increasing and should reach the value 1 at some point. The fed-up functions and attraction functions used are shown in Figure 3.

4.1.3 Node types

Each node can have exactly one of five different *types*: *home*, *workplace*, *shopping*, *hobby* and *empty*. Types are used to facilitate assignment of attraction and fed-up profiles: it is possible to simply flag a group of nodes as workplace nodes, and then set the attraction profile of all workplace nodes to be some function.

Another reason for using node types is that home and workplace nodes are fixed; each car is given a single home and a workplace node. Home and workplace nodes are special in the sense that each car is only attracted to its own home and workplace nodes; the attraction of other home and workplace nodes are always zero. However, several cars may share the same home and workplace nodes. Shopping and hobby nodes are not given for any car and these types of nodes will follow the standard rules mentioned above.

[3]Our simulation model uses Mersenne Twister [23], which is the default MATLAB® random number generator at the time of writing.

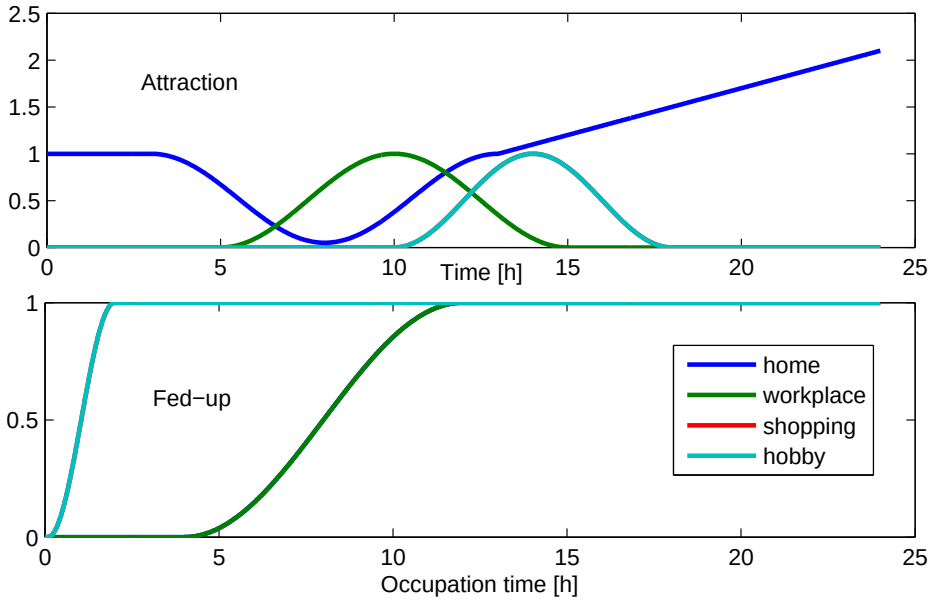

Figure 3: The control functions used in the simulations. Note that home attraction is always positive. The attraction function for shopping nodes is the same as for hobby nodes, the fed-up function for workplace nodes is the same as for home nodes and the fed-up function for shopping nodes is the same as for hobby nodes.

Empty nodes are nodes that have no attraction. Thus, no car will ever stop at an empty node. The empty nodes are used here to allow for more freedom in the creation of the node network.

4.2 Charging function

The charging function is a function that allocates the available energy each timestep between the cars connected to the grid. Because each node has its own available energy E_i, the charging function is evaluated separately for each node. The inputs to the charging function can be practically anything, for example the current SOC, capacity and a prediction for the amount of time the car will stay at the node. The output is a nonnegative real-valued vector W of size $N \times 1$, where N is the amount of cars connected to the node. The element W_c of this vector equals the *weight* of the car c i.e. how much this car is favored when allocating the energy. W is then scaled linearly so that the sum of its elements is 1. After this, each car attempts to receive energy

$$e_c = W_c E_i \tag{3}$$

If this energy cannot be received completely, for example due to battery reaching full capacity, the total overflowed energy is reallocated between the cars that are able to receive it using the charging function, but now with updated input values. This process is repeated until there are no cars

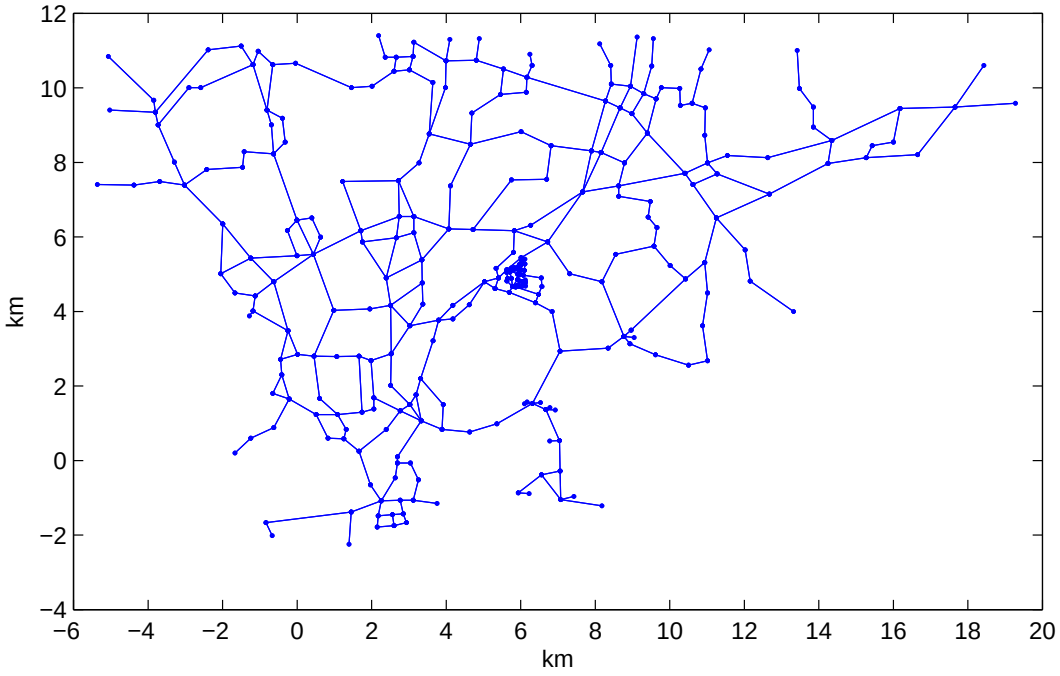

Figure 4: Helsinki node network used in the simulations.

left that can receive energy this timestep. At the next timestep, the weights are recalculated, now with updated parameters from the previous timestep.

4.3 Node network and the amount of cars

The setting of the simulations is Helsinki. A node network that represents an area of Helsinki was created, see Figure 4. The node types were chosen so that they would reflect the actual activities in the area reasonably well. The node types are shown in Figure 7.

After determining the node types, home nodes and workplace nodes were assigned for each car. This process was loosely based on the population and workplace data in [24]. The workplaces were assigned to each car randomly; there is no correlation between the location of the home node and the location of the workplace node. The amount of cars assigned to each home and workplace nodes is shown in Figures 5 and 6 as spheres.

Before any simulations are possible, a decision must be made on the amount of cars that will be simulated. Choosing a number too low results in charging profiles and travel length histograms being coarse, while having a large number of cars results in smoother profiles. Figures 8 and 9 show the cumulative travel histogram and the charging profiles with different amounts of simulated cars. In order to achieve greater prevalence, the resulting curves should be smooth, but having a large number of cars

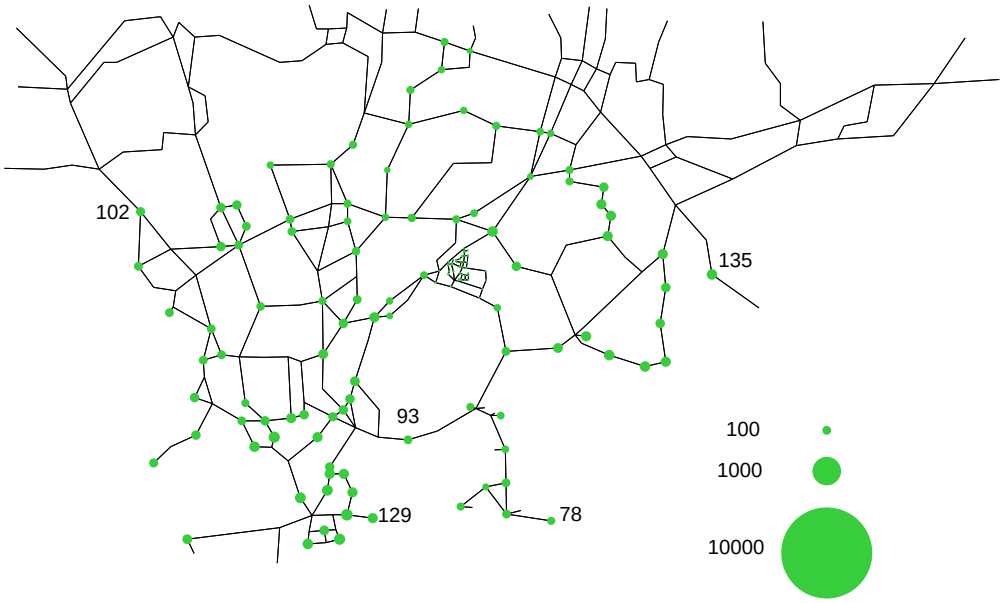

Figure 5: The amount of cars assigned to each home node. This amount is proportional to the area of the colored sphere on top of the home node. Three example spheres representing 100, 1000 and 10 000 assignments are also shown.

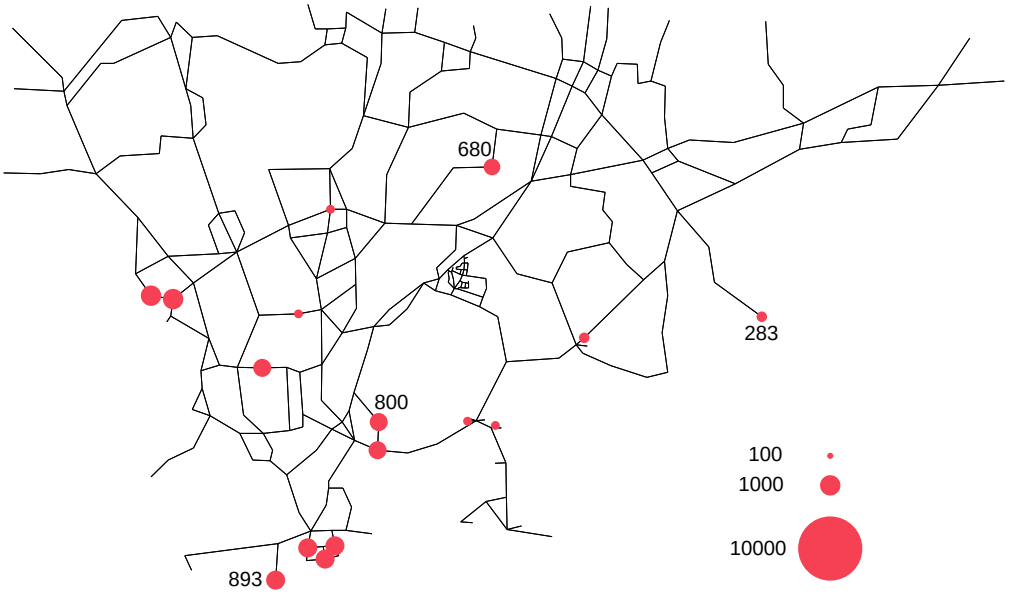

Figure 6: The amount of cars assigned to each workplace node.

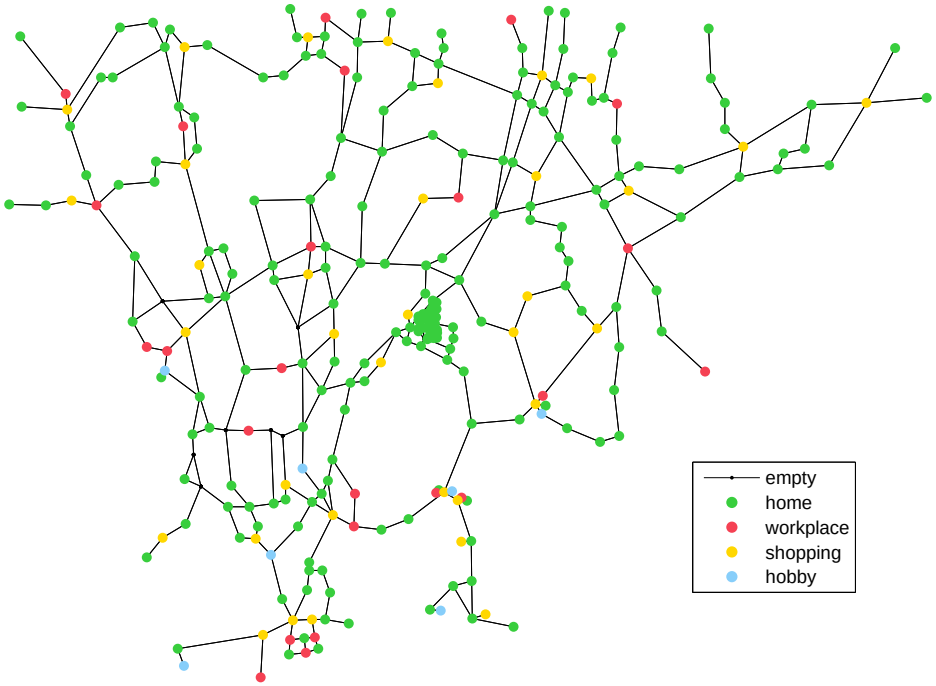

Figure 7: Node types.

requires more computation time. We made a compromise between these two objectives and chose to simulate 10 000 cars.

If the resulting charging profiles are reasonably smooth, it is possible to obtain charging profiles for larger amount of cars by interpreting that a single simulated car represents a fleet of a fixed number of cars and multiplying the profiles by the fleet size.

4.4 Resulting populations and time distributions

The chosen control functions yield the population profiles shown in Figure 11 and the travel length histogram shown in Figure 10. Total amount of kilometers driven is 243 687, yielding 24.4 km per car on average. Note that the total population does not equal 10 000 during all the timesteps. This is because when the cars are moving i.e. occupying transit space, they are not considered to be part of the population of any node.

Figure 12 shows the histogram for special events such as departure from home and arrival at the workplace. There is a clearly visible spike in the home leaving events at timestep 61. This is because there are cars with fed-up values larger than the fed-up factor at the home nodes that have no possible destination candidates due to the workplace attraction function being zero until timestep 61.

Figure 13 shows how these special timesteps correlate with each other. Note how the data points are divided in the subfigure showing the correla-

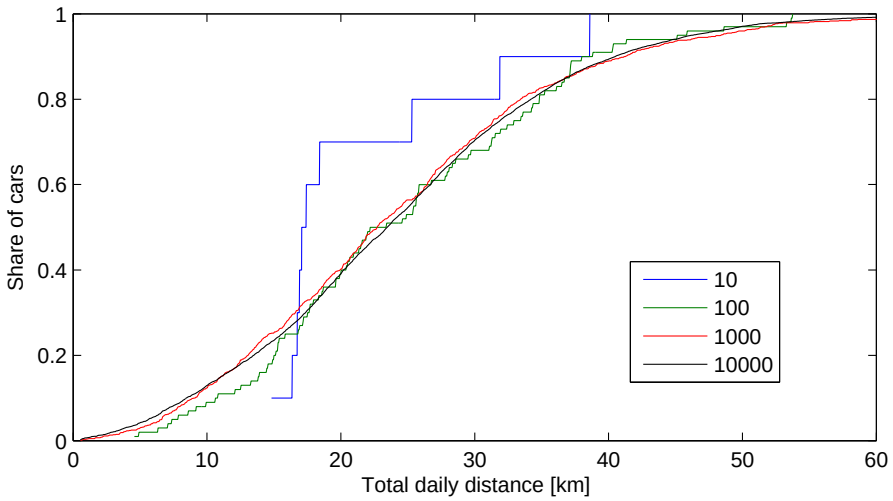

Figure 8: Cumulative travel histogram with different amounts of simulated cars.

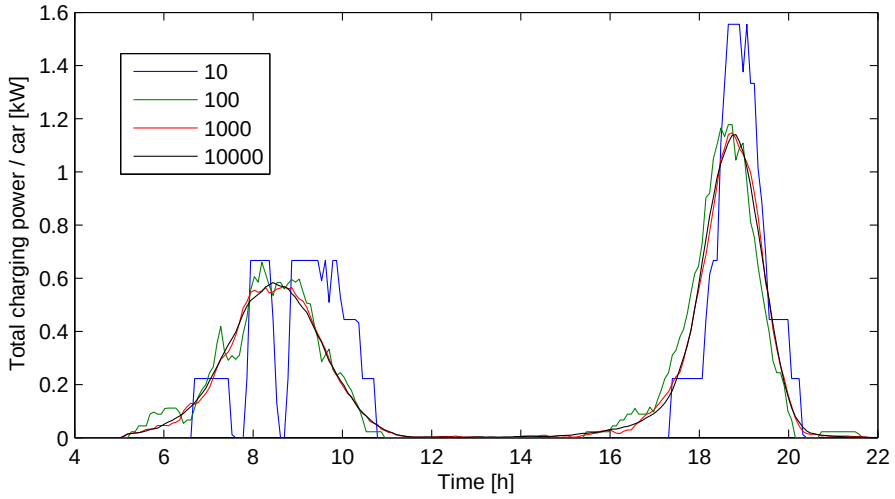

Figure 9: Charging profiles divided by the amount of simulated cars. The left-hand peak is due to workplace recharging and the right-hand peak due to home recharging.

tion between work leaving time and home arrival time. The linearly shaped cluster is generated by the cars that go straight home after work and the other cluster by the cars that go to shopping and hobby nodes on the way back. Also note that in the rightmost subfigure the home leaving time is accumulated horizontally at the timestep 61.

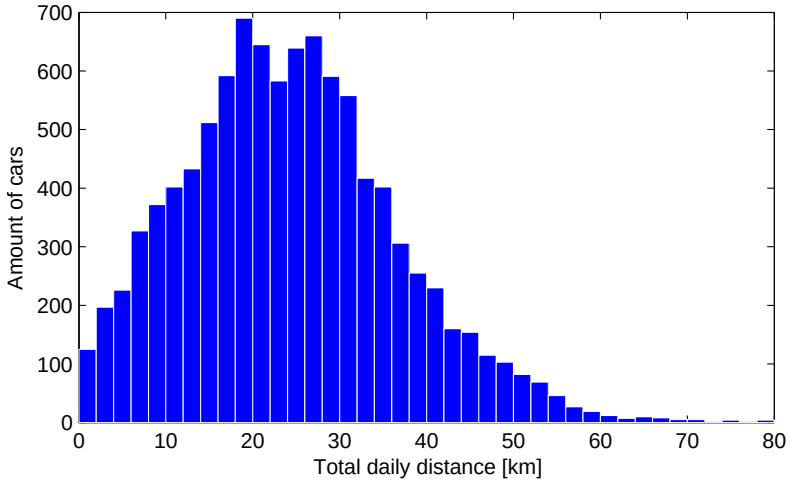

Figure 10: Travel distance histogram with 10 000 cars.

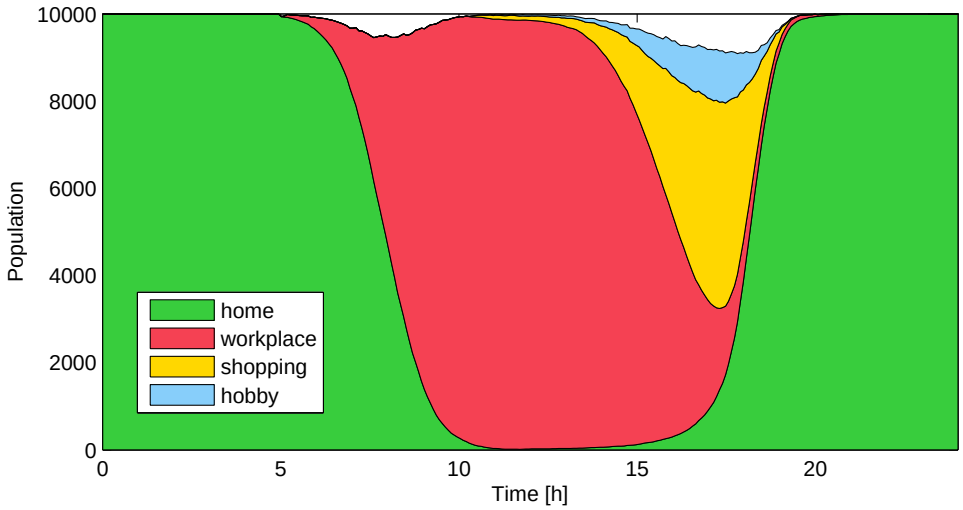

Figure 11: Population by node type versus time.

4.5 Power limitation

During high power consumption, the PHEVs are expected to react by providing demand response. This demand response is modelled by imposing a limitation to the vehicle recharging power. There are several different ways to limit the amount of available power for recharging.

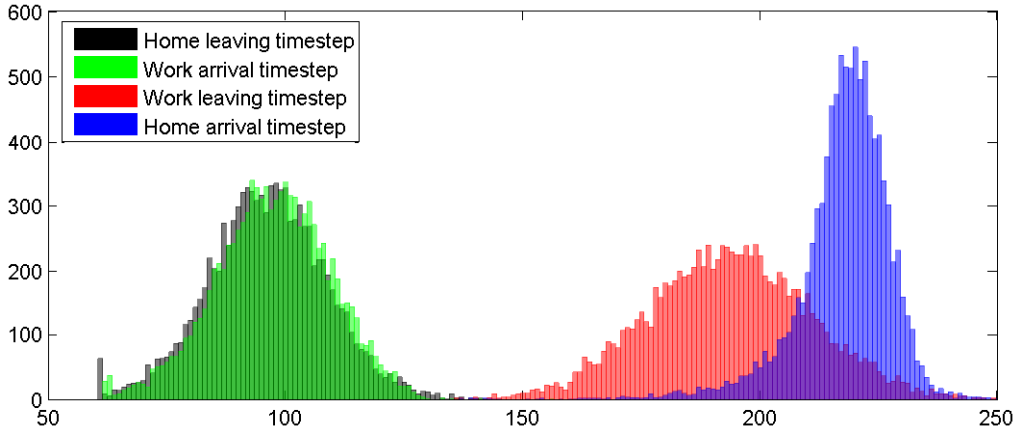

Figure 12: Distribution for home/workplace leaving/arrival timesteps. Home leaving timestep is the first timestep during which the car leaves its home node. Work arrival timestep is the first timestep during which the car arrives to its workplace (if it arrives at all). Work leaving timestep is the first timestep during which the car leaves its workplace node. Home arrival timestep is the first timestep during which the car arrives to its home node on the condition that it has occupied a different node during the previous timestep.

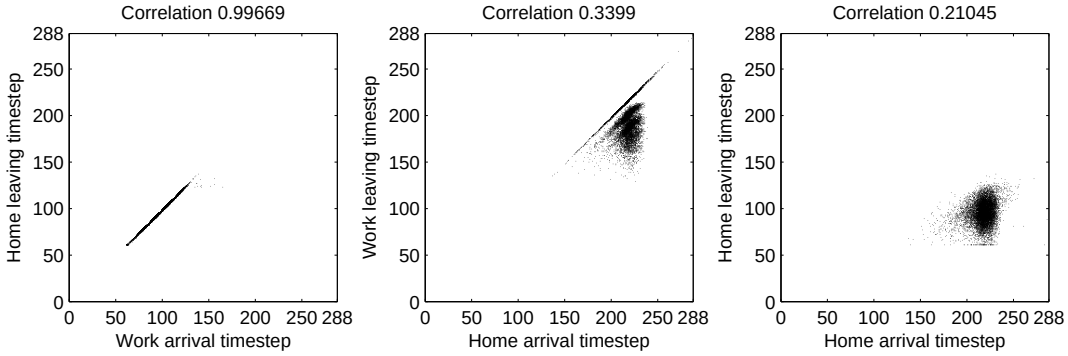

Figure 13: Time correlations that result from our choice of control functions.

4.5.1 Total recharging power

An intuitive way of limiting the charging power is to set a limit to the amount of total power a given node may dispense to the connected cars. We assume that the power grid is built with a good knowledge of the loads at different nodes so that workplace nodes that attract more PHEVs are better equipped to dispense charging power i.e. they support larger total charging power. This power limitation is carried out using a *power factor* p. This means that the total recharging power given by a node i is limited to

$$P_i = p \times N_i \tag{4}$$

where N_i is the *amount of inhabitants* at node i. The amount of inhabitants at home node i is equal to the amount of cars whose home has been set to

node i, while the amount of inhabitants at workplace node j is equal to the amount of cars whose workplace has been set to node j. Because of this, the amount of inhabitants is defined only for home nodes and workplace nodes and not for shopping and hobby nodes.

4.5.2 Charging socket

The power factors only limit the node's total recharging power, not the recharging power for individual cars or the charging sockets via which cars are connected to the grid. This means that if there are no power limitations for the cars or sockets, a single car at node i might recharge with power P_i, which can be very (unrealistically) large. Therefore, it is assumed that the power limitation for one socket is 7.4 kilowatts[4]. It is further assumed that the efficiency of recharging is 0.9. This implies that no car may increase its battery energy level faster than 6.66 kilowatts.

4.5.3 Battery

In addition to these two power limiters (node total and socket), it is possible to use a car-specific power limiter to model the maximum supported recharging power of the battery. For now, however, we assume that each battery supports infinite recharging power.

4.5.4 Home node recharging

The power in home nodes is not limited unless otherwise mentioned. Power limitations are expected to be feasible mainly during the day, when the base power consumption is high, and not during the night, when the base consumption is low.

Importantly, when the home nodes support infinite total recharging power, all cars are likely to be fully recharged during the night. If the car is occupying the home node for nine hours (Figure 11), it is capable of receiving 9 h $\times$ 6.66 kW $\approx$ 60 kWh of energy. Because the battery capacities that will be used are much smaller than this, it can be safely assumed that each car reaches maximum SOC at home. This enables beginning the simulation with full SOC for each car while maintaining consistency. If the total home recharging power is limited, there may be need to repeat the simulation until the SOC's converge, which would increase the computation time considerably.

4.5.5 Shopping node and hobby node recharging

For simplicity, it is assumed that recharging is only possible at home and at workplace. This is implemented by setting the socket power limiter in all shopping and hobby nodes to 0 kW.

[4] 230 volts at 32 amperes, alternating current.

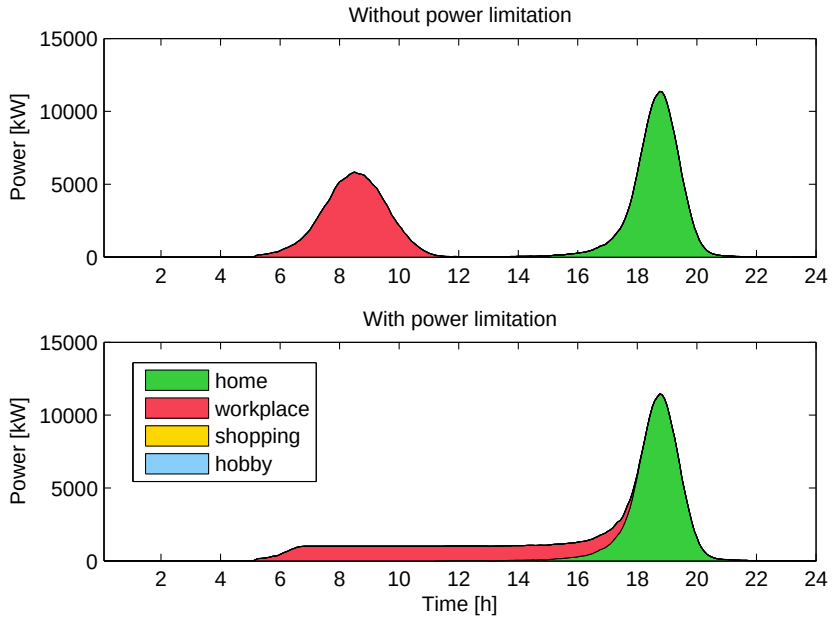

Figure 14: Charging profile with and without power limitation at workplace nodes. The workplace power factor is infinite in the above picture and 0.1 kW in the below picture.

4.5.6 Effect of power limitation

Figures 14 and 15 show the effect of this power limitation on the power consumption profile and the integral of the consumption profile, respectively. Note how, in the end of the simulated day, the total energy used in home nodes is larger than the total energy used in workplace nodes. This follows from the choice of the control functions as discussed in section 5. Also note how the total energy used in the end of the day is larger in the non-throttled case.

The effect of different workplace power factors and capacities on the electric kilometers using the null-strategy is shown in Figure 16. It is seen that the effect of increasing the power factor saturates at some point. This is sensible, because the amount of electric kilometers cannot be increased past the total kilometers travelled. This saturation also happens when increasing the battery capacity, as was already seen in Figure 1. Note how the power factor has less effect with very big and very small capacities. When the batteries are sufficiently large, the cars do not need workplace charging in order to avoid using fuel on the way home. If there is no fuel consumption, there will be no difference in the electric kilometers. When the batteries have small capacity, they will be able to recharge fully even with small power factors. In this thesis, the workplace power factor of 0.1 kW is used unless otherwise mentioned.

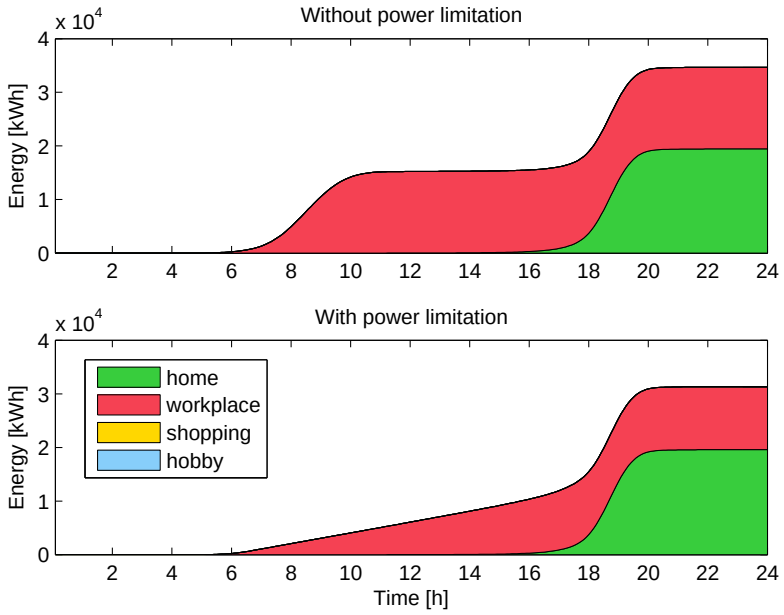

Figure 15: Integral of the charging profile with and without power limitation at workplace nodes. The workplace power factor is infinite in the above picture and 0.1 kW in the below picture.

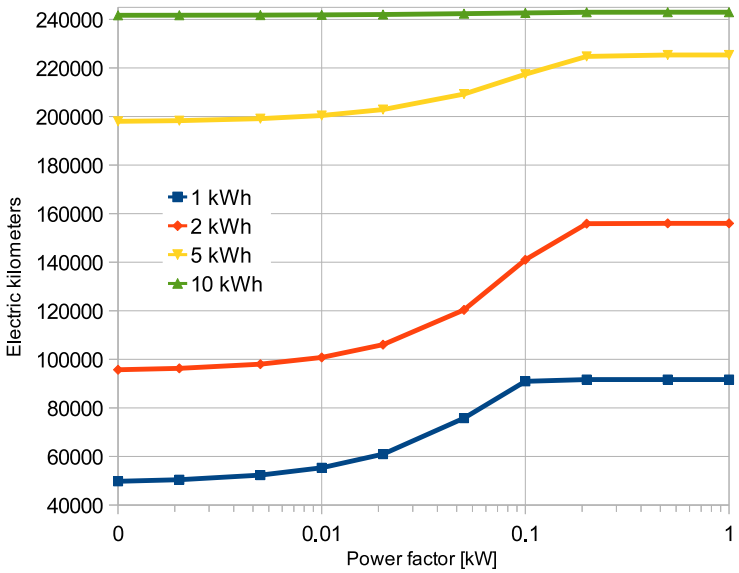

Figure 16: The relationship between workplace power factor and capacity.

5 Workplace charging

Different strategies for workplace charging are studied first. This section has been divided into three subsections. In the first section, only the information based on the current SOC and capacity of a battery is used. In the second section, we additionally use information about the departure time and the next free distance of the car. The second section therefore contains predictions of the future, while the first one does not. The utility of having charging strategies for the workplaces is studied in the final section. These strategies have no effect at home nodes, because the power factor at home nodes is infinite.

It should be noted that the length of the trip home is always greater than or equal to the length of the trip to work. This is the result of the attraction functions chosen: when the car leaves the home node in the morning, the only possible destination is the workplace node, for only the workplace node has a nonzero attraction. In the case of leaving the workplace node, shopping and hobby nodes have nonzero attraction allowing the car to make a "detour". Thus each packet of energy that is given to the cars recharging at the workplace is used with 100 % probability on the way home. It is therefore impossible to waste energy directly by recharging a car too much. However, it is possible to waste energy *indirectly* by ignoring the fact that some cars leave the node earlier than others i.e. not giving the energy to a higher priority car.

5.1 Non-predictive strategies

The charging strategies in this section do not make any predictions about the future, making only use of the current situation characterized by two parameters: the SOC and capacity. Strategies based only on SOC are studied first. Capacity is then added to the charging functions to see its effect on the results. In the case of different capacities, we study both the case where there is no correlation between capacity and travelled distance and the case where this correlation exists.

5.1.1 SOC-based strategies

Every PHEV or EV needs to know its current SOC in order to prevent damage to the battery and therefore information about SOC is practically always available for all cars that are plugged in, assuming that the car is able to communicate this information to the utility.

Three simple strategies are studied first, by using a charging function of the form:

$$z_1 = \exp(\alpha x) \tag{5}$$

where x is the normalized SOC (real number between 0 and 1). The three strategies are obtained by changing the value of the parameter α:

- $\alpha = -30$: *favor low-strategy*
- $\alpha = 30$: *favor high-strategy*

- $\alpha = 0$: *null-strategy*

For example, if $\alpha = -30$, low-SOC cars will be favored over high-SOC cars, because smaller x are penalized less by the charging function, thus giving them more weight.

Figure 17 shows what kind of effect the strategies have on the SOC curves and the kilometers travelled using electricity. Using the null-strategy, the car represented by the thick green line, the "green car", is not recharged sufficiently because its SOC drops to zero during timestep 221. This implies that the car has to use fuel to cover the remaining distance. When the favor low-strategy is used, the green car receives more energy due to having a lower SOC than the rest of the cars on the node. With this extra energy the SOC of the green car never drops to zero. Actually, none of these SOC curves drop to zero with this strategy. With the favor high-strategy, the green car receives *less* energy than the other cars and produces more fuel kilometers than with the null-strategy.

Favoring some cars over others may lead to the non-favored cars having a lower SOC than with no favoring. This can be seen from the SOC of the car represented by the thick light blue line, the "blue car": when comparing the null-strategy and favor low-strategy, it is seen that favoring the green car shifts the SOC curve of the blue car downwards. Also, if the green car is not a high-priority car, it is possible to favor it excessively, generating more fuel kilometers than in the case where a more sensible favoring is used.

5.1.2 Adding capacity

Information on the battery's capacity is also almost always available. The capacity is included into the previous strategy in two different ways: by favoring the cars with high maximum capacity and penalizing the cars with high maximum capacity.

In order for the addition of capacity to make sense, cars with different battery capacities are required. This is done by randomly picking 25, 50 and 75 % from the total of 10 000 cars to have a battery capacity of 6 kWh, while the rest of the cars will have 2 kWh batteries. Three different charging functions are used:

$$\begin{aligned} z_1 &= \exp(-30x)y \\ z_2 &= \exp(-30x)/y \\ z_3 &= \exp(-30x) \end{aligned} \tag{6}$$

where x is as before and y the battery capacity in kWh. Note that we have chosen to modify the favor low-strategy, for it seems the most promising.

The results are plotted in Figure 18. It seems that these strategies have only a marginal effect on the electric kilometers. The biggest difference in electric kilometers, 1034 km, occurred between strategies z_2 and z_1 when 50 % of the cars were 6 kWh.

It is natural to expect larger batteries to support higher charging power. To see how this would affect the results, we assume that when there are no power limitations, the shortest time for a battery to recharge from empty to full is 30, 60, 120, 240 and 480 minutes and independent of battery size.

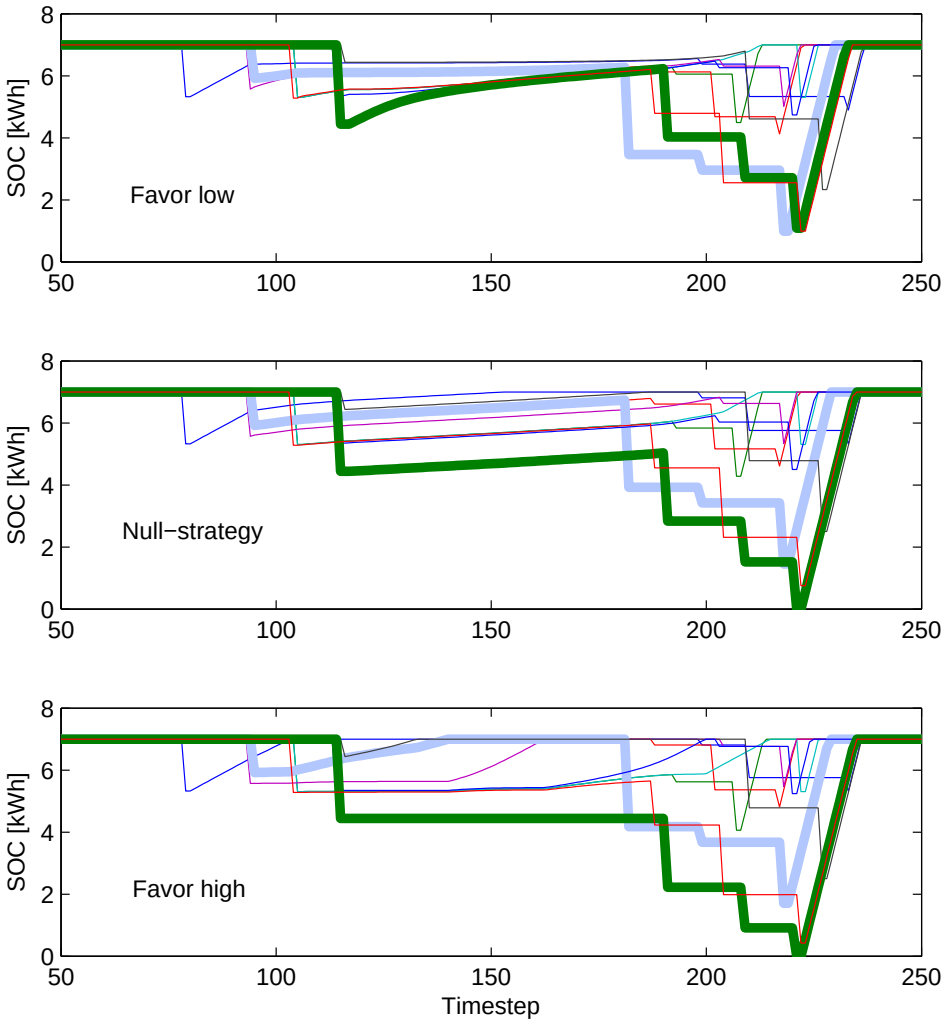

Figure 17: SOC curves using three different charging functions. The SOC drops rapidly in the Figure because all the energy the car will use during its trip is reduced at the departure timestep. This is done in order to facilitate computation.

This means that the maximum charging power supported by the battery in kilowatts is

$$P = \frac{y}{m/60} \tag{7}$$

where y is the capacity in kilowatt-hours and $m \in \{30, 60, 120, 240, 480\}$. Here it is assumed that 50 % of the cars have 6 kWh batteries and 50 % have 2 kWh batteries. The results are plotted in Figure 20. It is seen that, even after using a lower charging power for smaller batteries, it is more effective to favor the smaller batteries.

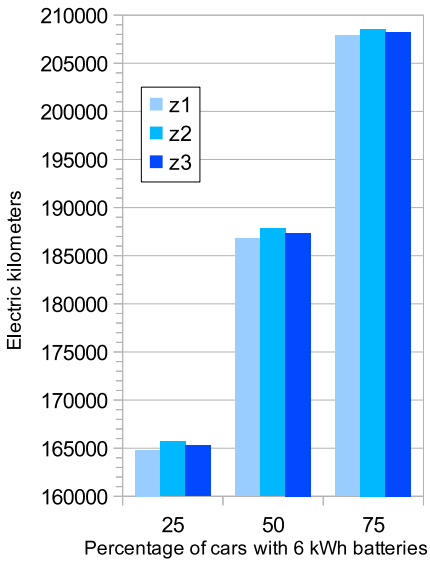

Figure 18: Electric kilometers using strategies z_1, z_2 and z_3 with different percentages of cars with large batteries (i.e. big factors).

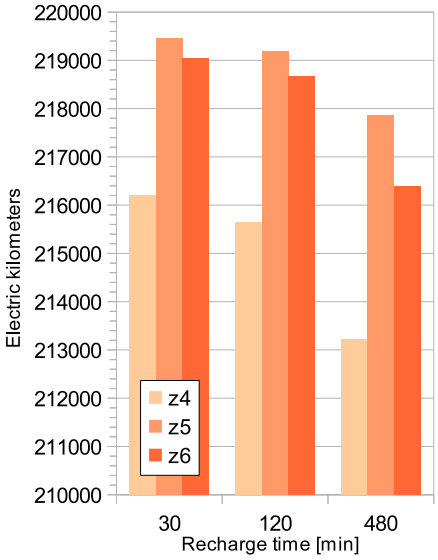

Figure 19: Electric kilometers using strategies z_4, z_5 and z_6 with different recharge times (independent of capacity). SOC is ignored, DCC is enabled, big factor is 50 %.

However, smaller batteries tend to run out more quickly, which causes them to have a lower SOC on average, which in turn grants them more charging power bandwidth due to the form of the charging function. It will now be checked if disabling SOC-based favoring will affect the results.

5.1.3 Strategies based on capacity only

Unless otherwise mentioned, it is from now on assumed that the maximum recharging power supported by the battery is calculated using (7), with $m = 60$.

Three different strategies are tested:

$$\begin{aligned} z_4 &= y \\ z_5 &= 1/y \\ z_6 &= 1 \end{aligned} \tag{8}$$

Note that strategy z_6 corresponds to the null-strategy. The results are shown in Figure 20.

As is evident by the figure, ignoring the SOC and completely focusing on the capacity does not affect the observation that favoring small capacities leads to bigger electric kilometer gain. There is at least one more thing that should be taken into consideration: the correlation between high battery capacity and distance driven. For simplicity, a binary model is used for this correlation. This means that the correlation is either enabled or disabled, with no intermediate configurations.

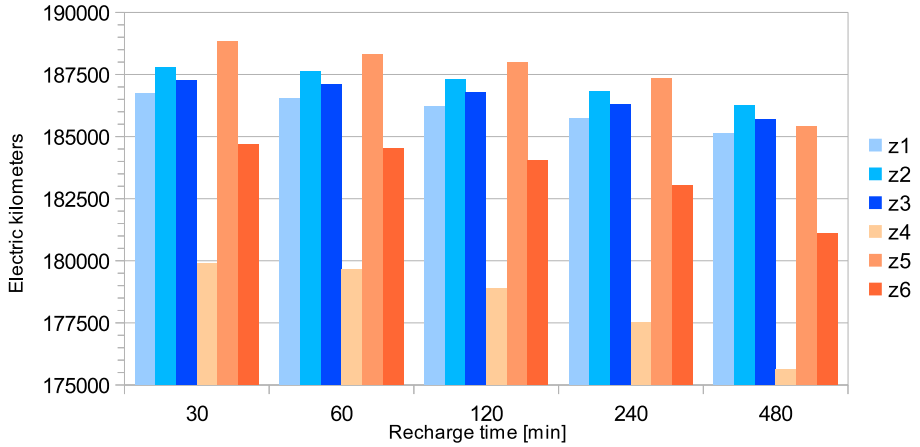

Figure 20: Comparison of the strategies that favor low-SOC cars (z_1,z_2,z_3) and strategies that ignore SOC (z_4,z_5,z_6). Battery sizes are 2 kWh and 6 kWh with big factor 50 %. DCC is disabled.

5.1.4 Distance-capacity correlation, DCC

Before this, no correlation was assumed between high battery capacity and long travel distances; the cars that would have larger 6 kWh batteries were chosen randomly. It is now checked if enabling *distance-capacity correlation*, or DCC, would have any significant effect on the results. Correlation is implemented as follows:

1. One simulation is run to obtain the total kilometers driven by each car. Battery sizes are arbitrary at this point because they do not affect the kilometers driven.

2. A certain fraction of the cars, given by the *big factor*, with the biggest amount of total kilometers driven are selected to have a larger battery. The remaining cars will receive the smaller battery. Here the big factor of 50 % is used.

3. The random number generator is reset so that car movement in the next simulation will be identical to the car movement in the first simulation.

4. Simulation is run again with the new battery sizes.

The results are shown in Figure 19. Favoring low capacities still remains the best strategy. Note that the electric kilometers increased in most cases compared to Figure 20.

5.1.5 Optimal weight for the SOC

Three findings have been made:

- When there are low-SOC and high-SOC cars with the same capacities, it is often better to favor the low-SOC cars.
- When there are low-capacity and high-capacity cars and SOC is ignored, it is better to favor the low-capacity cars.
- In some cases, it is better to favor the low-SOC cars and in some cases, it is better to ignore SOC, as seen in Figure 20.

These findings suggest that there exists an optimal strategy between the two extremes (only focus on SOC / only focus on capacity). With the charging function being of the form

$$z = \exp(\alpha x)/y \tag{9}$$

we search for the value of weight parameter α that produces the most electric kilometers. The results are shown in Figure 21. The curves are labeled using the abbreviation "RTtBFbc", where "RT" is a short for *recharge time*, t is the recharge time in minutes, "BF" is a short for *big factor* and b is the big factor in percents. "c", short for *correlation* is included in the label if and only if DCC is enabled. Curves labeled with the prefix "null-" refer to the case where the null-strategy is used.

It is seen that, without DCC, it is best to slightly favor the low-SOC cars. With correlation, it is best to slightly favor the high-SOC cars. A possible explanation for this reversal is that, due to the correlation, the cars with high capacity are more likely to travel long distances and due to the high capacity, their normalized SOC is expected to be high at the workplace. Note that this is not contradictory, as the large batteries are given to cars with the longest *total* travel length, not the longest trip length from home to work. Because most of the travelling occurs on the way home, these cars should be favored slightly.

When DCC is enabled, the null-strategy kilometers are exceeded only with big factor 50 %. With big factors 25 % and 10 % the results are worse than with no strategy at all. It would seem that this form for the charging function is impractical when DCC exists.

From Figure 21 it can also be seen that:

1. The electric kilometers approach nearly asymptotically a certain value when $|\alpha| \to \infty$.
2. The global optimum is always near zero or at $\alpha = -\infty$. The global minimum is always at $\alpha = +\infty$.
3. The difference between the values at $\alpha = \pm\infty$ decreases when distance-capacity correlation is included.
4. Increasing the amount of cars with big batteries increases the difference between the asymptote values at $\alpha = \pm\infty$.
5. The global maximum seems to be on the positive side only when the correlation is included.

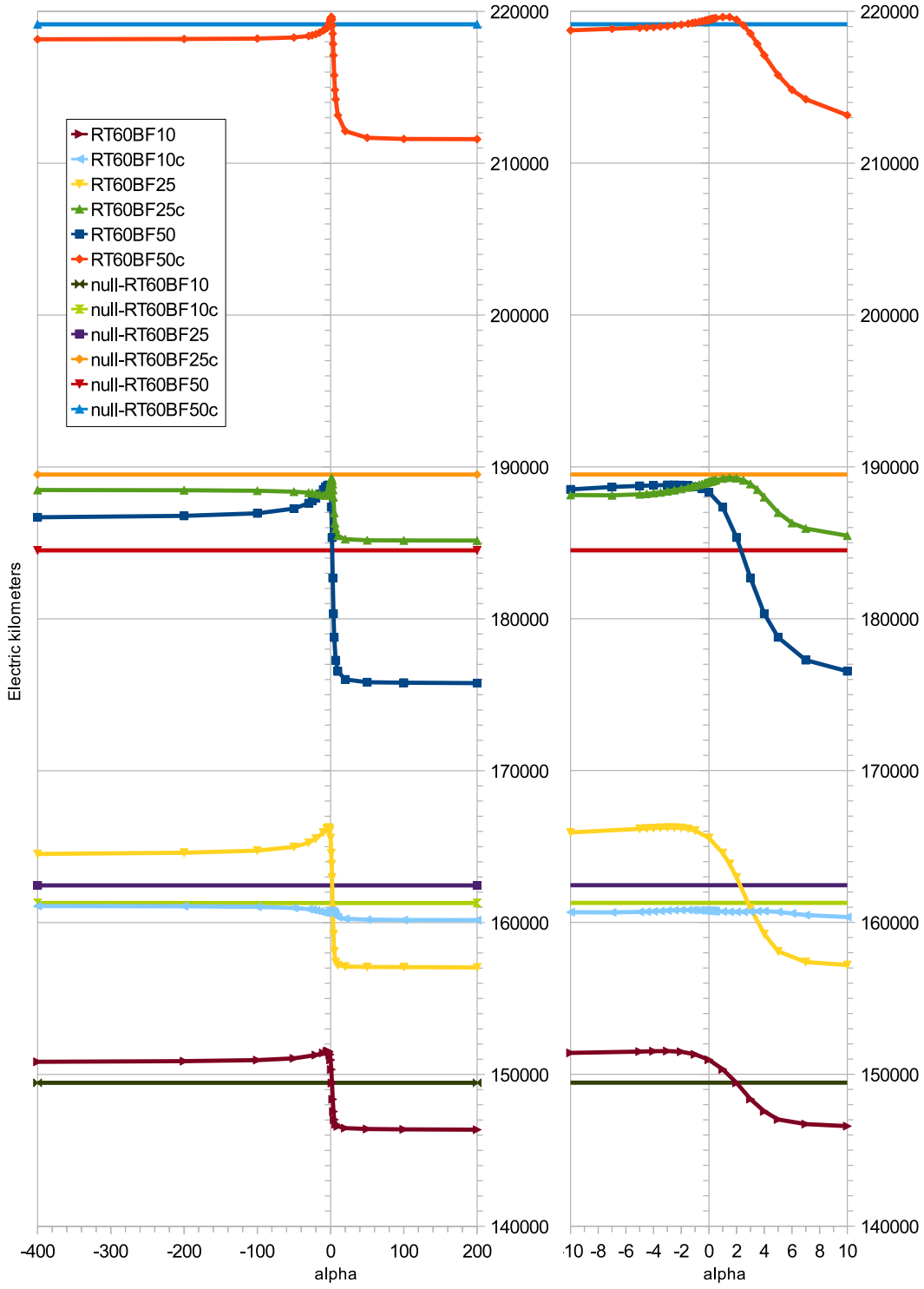

Figure 21: Electric kilometers as a function of weight of SOC α using the charging function in (9) with different cases. The right-hand figure is a zoomed-in version of the left. For label explanations, see section 5.1.5.

The first result is sensible, because both the amount of electricity that can be wasted by excessively favoring low-priority cars and the energy that can be used to move the cars are upper-bound.

Favoring high-SOC cars too much rapidly increases the amount of wasted energy. Favoring low-SOC too much is safer because of the reduced probability of bandwidth being hogged from high-priority cars.

The intuitive explanation for the third result is that, because the difference between the two asymptote values is caused by low-priority cars hogging the bandwidth from high-priority cars, the priority difference is decreased by the introduction of DCC.

With more total capacity, there are more possibilities of hogging the charging bandwidth from high-priority cars and (to some extent) more possibilities to increase the electric kilometers. This explains the fourth result.

The fifth results is explained by the fact that increasing the correlation decreases the probability of hogging bandwidth from high-priority cars. Favoring high-capacity cars too much, however, results in great electric kilometer losses.

To rule out the possibility that the electric kilometer peak is caused by having two different capacities (2 kWh and 6 kWh) in the system, a simulation was run with big factor set to zero i.e. a simulation where all the cars had 2 kWh batteries. The results are shown in Figure 22, from which we see that the peak is still present.

When this local maximum is also the global maximum, it follows that it is possible to favor the low-SOC cars too much. If this were not the case, the global maximum would always be at $\alpha = -\infty$, because this implies that all of the available power is first given to the car with the lowest SOC, or several cars if they have the same lowest SOC.

A sensitivity analysis was performed for these results by changing the recharge time and the capacity of the big battery. This analysis is discussed in section 5.1.6.

5.1.6 Sensitivity analysis

Recharge time was decreased from 60 min to 30 min and increased to 120 min in the case where 50 % of the cars had 6 kWh batteries, with no DCC. The results are shown in Figure 23. The main difference is that the electric kilometer curve is shifted downwards when recharge time is increased and upwards when it is decreased. The shift (both up and down) is more pronounced on the positive side.

The large battery size was adjusted from 6 kWh to 4 kWh and 10 kWh so that the ratio between the big capacity and small capacity changed from 3:1 to 2:1 and 4:1. The results are shown in Figure 24. Besides the obvious increase in electric kilometers (which is upper-bound, as seen from Figure 1), it is seen that the drop near $\alpha = 0$ is amplified when the large battery capacity increases. The reason for this is that the upper bound for wasted electricity is shifted upwards i.e. it is possible to hog more bandwidth from the high-priority cars if a bad strategy is used.

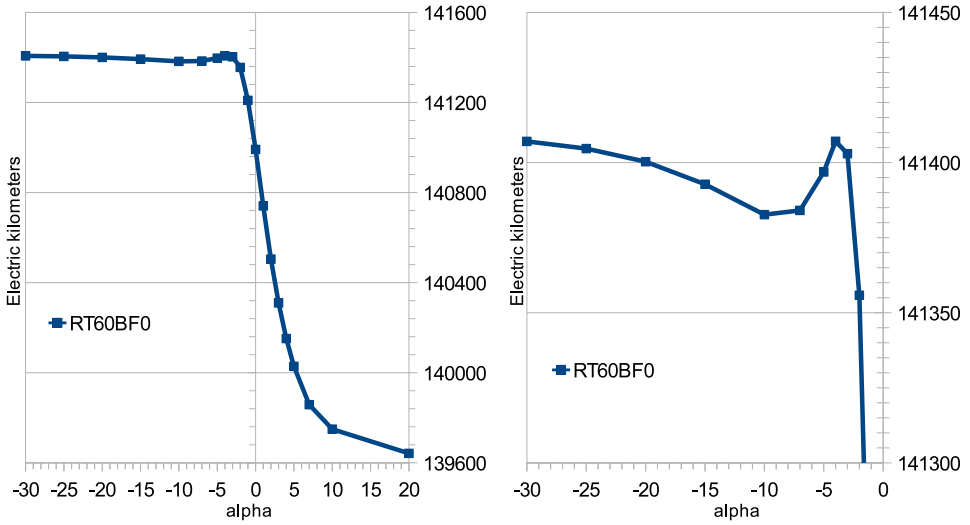

Figure 22: Electric kilometers as a function of weight of SOC α using the charging function in (9). Recharge time is 60 minutes, big factor is 0 %. The right-hand figure is a zoomed-in version of the left.

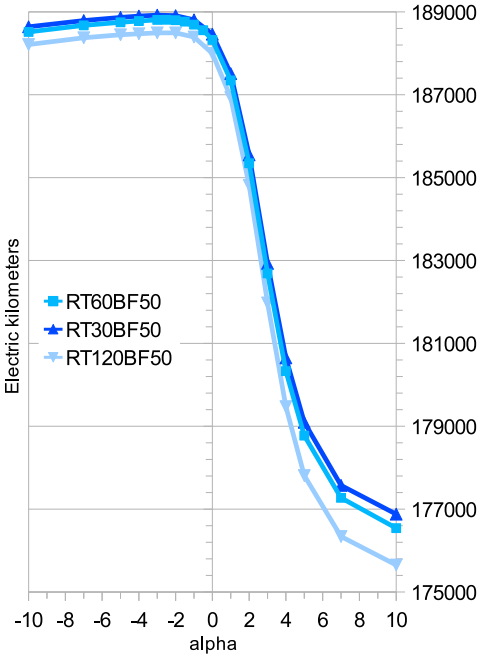

Figure 23: Sensitivity analysis for the charging function in (9), recharge time varying between 30 to 120 minutes. For label explanations, see section 5.1.5.

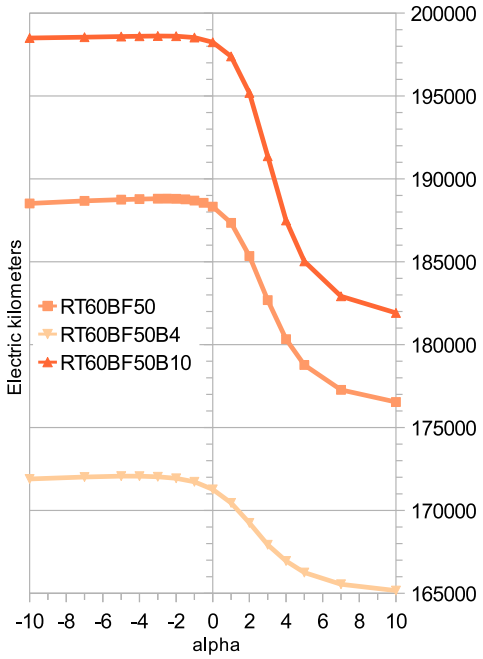

Figure 24: Sensitivity analysis for the charging function in (9), large battery capacity varying between 4 (label ending with "B4") and 10 kWh (label ending with "B10"). For additional label explanations, see section 5.1.5.

5.1.7 Energy-based strategies

Until this point, the (normalized) SOC and capacity have been kept separate from each other in the sense that their respective variables, x and y, have been separate in the control functions used thus far. However, it is also possible to combine them together as multiplying them yields the amount of energy E that can be extracted from the battery in kilowatt-hours. Experiments were made with the following strategy:

$$z = \exp(\alpha x y) = \exp(\alpha E) \tag{10}$$

with different values of weight parameter α. The results are shown in Figure 25, where the labels beginning with "E." refer to the energy-based strategy. The sensitivity of electric kilometers with respect to the weight parameter is clearly greater in the energy-based approach. This is expected, because the range of the value in the argument of the exponent function is increased from $[0,1]$ to $[0,6]$, the large battery capacity being 6 kWh.

In this figure, when using the energy-based approach the maximum is located in both correlated and non-correlated cases on the negative side of the x-axis while in the SOC and capacity-based approach the maximum is on the left side in the non-correlated case and (sometimes) on the right side in the correlated case. This raises the question: can the maximum occur with positive values of α when the charging function is energy-based? To answer this, a case where there was a very low probability of giving too much bandwidth for high-energy cars was chosen: the case where 10 % of the cars had 6 kWh batteries, with travel distance-capacity correlation. The results are shown in 26. The maximum clearly occurs on the positive side of the x-axis and thus the possibility that the positive α-maxima exist only when using SOC and capacity-based charging functions can be ruled out.

Because the left plateau in RT60BF50 is higher in the energy-based approach, it would seem that when there is no travel distance-capacity correlation, it is better to use the energy-based charging function. To check if this hypothesis holds, a simulation of RT60BF10 with both approaches was run. The results are shown in Figure 27. It is seen that the energy-based approach fares better on the negative side of the x-axis.

In all four cases (RT60BF10/c and RT60BF50/c), the energy-based charging function yielded greater maximum electric kilometers, suggesting that this form is closer to the optimal form for the charging function.

5.1.8 Linear combination of SOC and capacity in the argument of the exponential function

Experiments were made with the following charging function:

$$z = \exp\left(\lambda x + \eta y\right) \tag{11}$$

where λ is the weight of SOC and η is the weight of capacity. Battery capacities were set to 2 kWh and 6 kWh with big factor 50 %. The electric kilometers with different λ and η are shown in Figure 28, along with the electric kilometers obtained using the null-strategy. It is seen that in the case with no DCC, both λ and η should be negative to obtain more electric

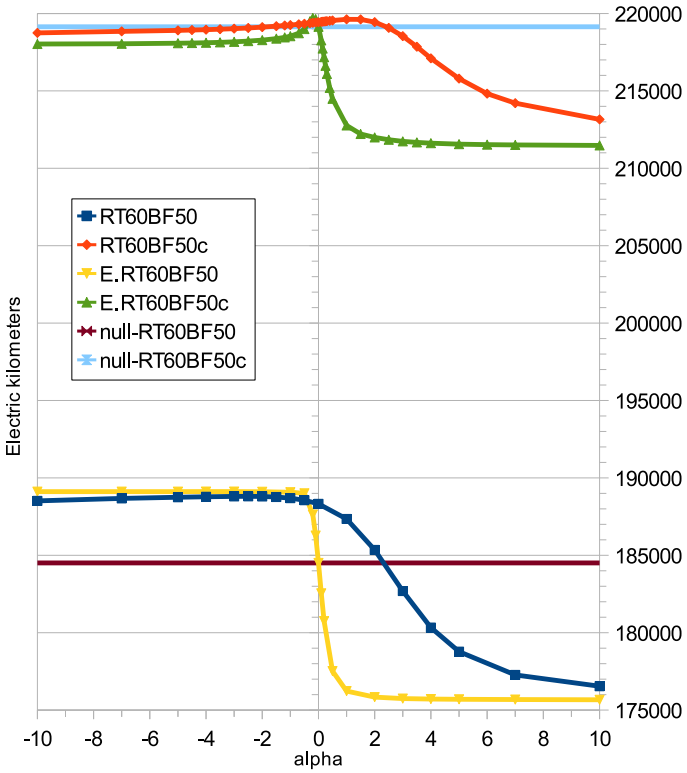

Figure 25: Electric kilometers as a function of parameter α using the charging functions (9) and (10). For label explanations, see sections 5.1.5 and 5.1.7.

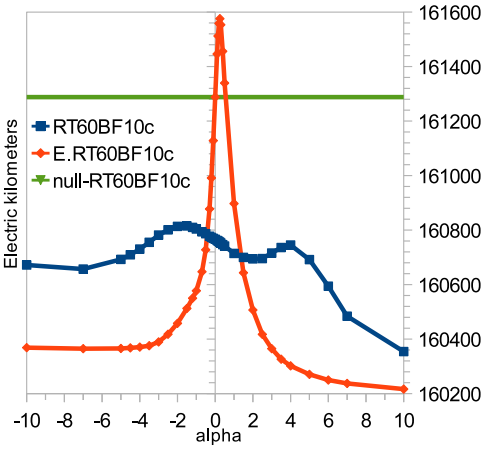

Figure 26: Electric kilometers as a function of parameter α using the charging functions in (9) and (10). For label explanations, see sections 5.1.5 and 5.1.7.

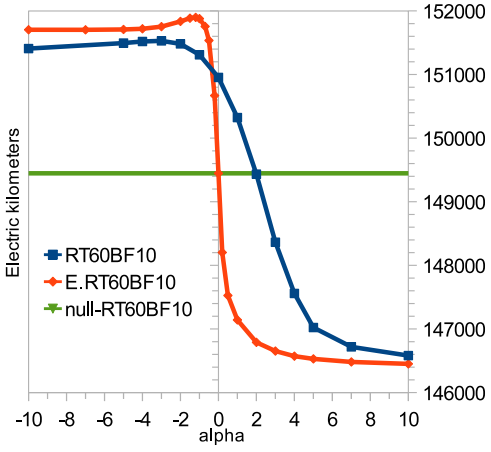

Figure 27: Electric kilometers as a function of parameter α using the charging functions in (9) and (10). For label explanations, see sections 5.1.5 and 5.1.7.

kilometers. Setting both positive is counterproductive, as we would then do worse than with the null-strategy. To obtain the most electric kilometers with this strategy in the case with no DCC, both λ and η should be set to a high value, to around $\lambda = \eta = -50$. The gain compared to the null-strategy case is around 4600 km.

With DCC enabled, a local maximum emerges. The optimal value of λ is dependent on η, and vice versa. The relationship of the two is shown in Figure 29. With this resolution and configuration, the optimal values are $\lambda = -1$ and $\eta = -0.1$. Using these weights the gain is only 575 km compared to the null-strategy case. Thus, as before, enabling DCC reduces the effectiveness of the strategy.

5.1.9 Linear charging function

The charging functions used thus far have all employed the exponential function. Experiments will now be made on the following, linear charging function:

$$z = \hat{y} - xy + \alpha(1-x) + \beta y \tag{12}$$

where $\hat{y}$ is the biggest capacity in the system (6 kWh), x and y are as before and $\alpha, \beta > 0$ are weight parameters. The small capacity is again 2 kWh. xy equals the available energy E in the battery. Note that because of $\hat{y}$ the charging function can never attain negative values.

The simulation was run using this charging function with different weight parameters α and β, with and without DCC. The results are seen in Figure 30.

In the case with no DCC, it seems that increasing both α and β reduces the electric kilometers. If this is the case, both weight parameters should be set to zero for maximal utility. The utility gain compared to the null-strategy is then around 4400 km.

If DCC is enabled, the situation changes: we see that there exists a positive optimal value for the weight of capacity β that is dependent on the weight of SOC deficit α. The electric kilometer peak is shifted to the right when α is increased. This is because a larger β is required to balance the increased influence of α. However, it seems that the global optimum cannot be attained with positive values of α due to bad 1:α:β -ratio. Maximum utility is gained with weights $\alpha = 0$ and $\beta = 0.2$, but this is only around 440 km larger compared to the null-strategy case.

The peak is present, though smaller in height, even with very large values for the weight of SOC deficit ($\alpha = 10000$). It would seem that the peak cannot be eliminated using finite values for this parameter.

5.2 Predictive strategies

Until this point, the strategies we have used have relied only on the knowledge of the current SOC and capacity. Now two new variables are introduced, the *stationary time* T, which is the time of departure from the current location minus current time and the *next free distance* D, the distance the car will travel between leaving the current node and reconnecting with

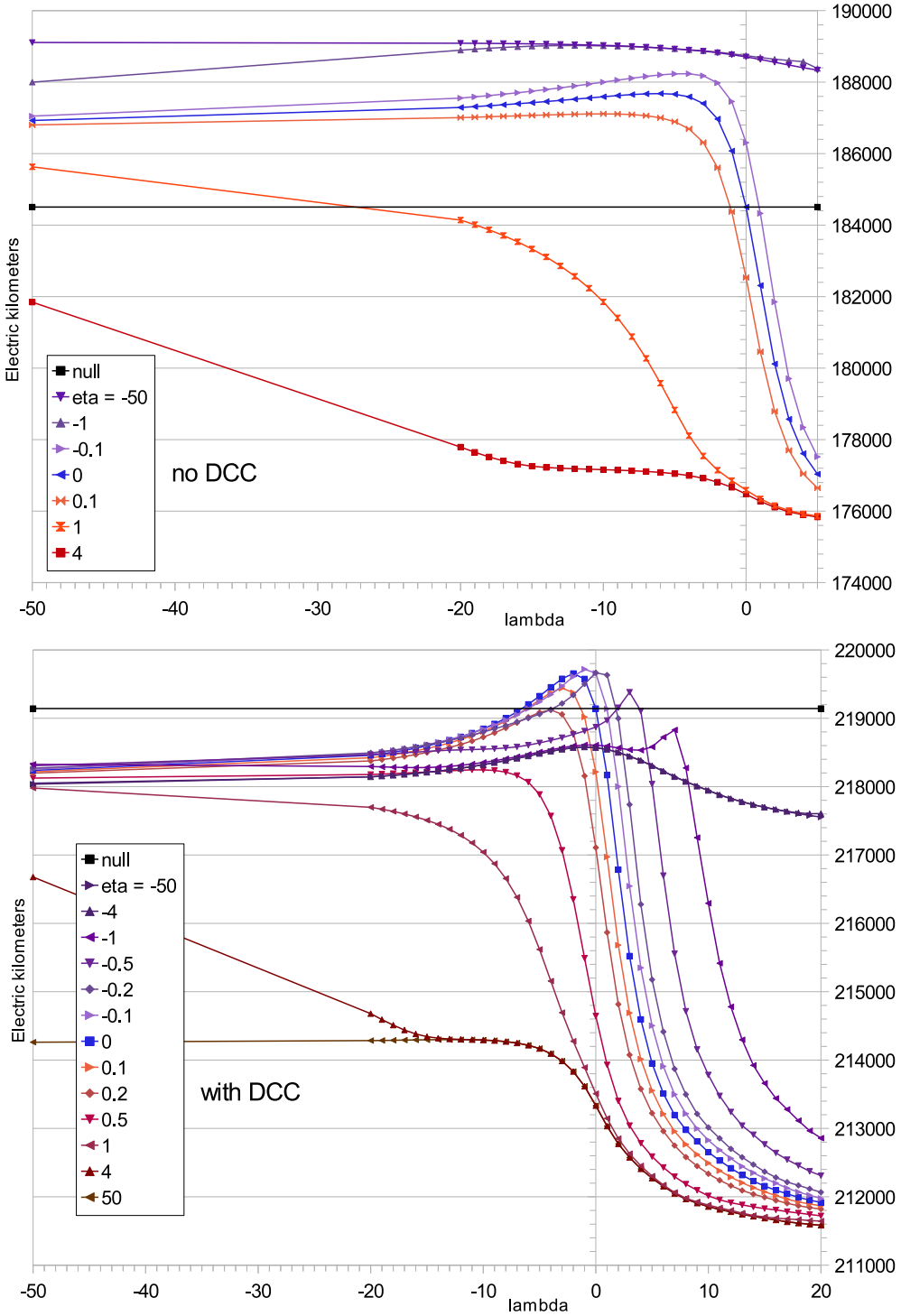

Figure 28: Electric kilometers with different weight of SOC λ and weight of capacity η using the charging function in (11), with and without DCC. Battery capacities are 2 kWh and 5 kWh, big factor is 50 %. The curve labeled "null" shows the amount of electric kilometers obtained using the null-strategy.

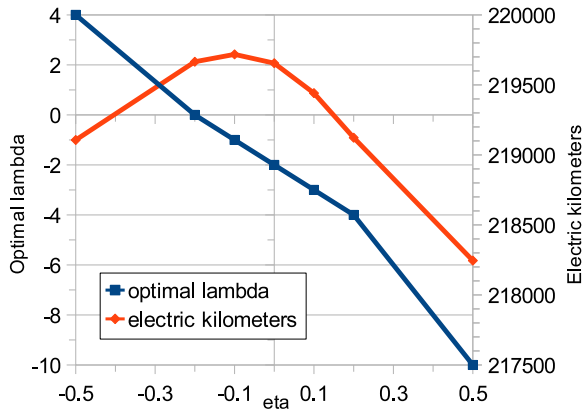

Figure 29: Optimal values of weight of SOC λ that maximize the electric kilometers as a function of weight of capacity η, extracted from Figure 28 (the case with DCC). Also showing the electric kilometers obtained with optimal values of λ.

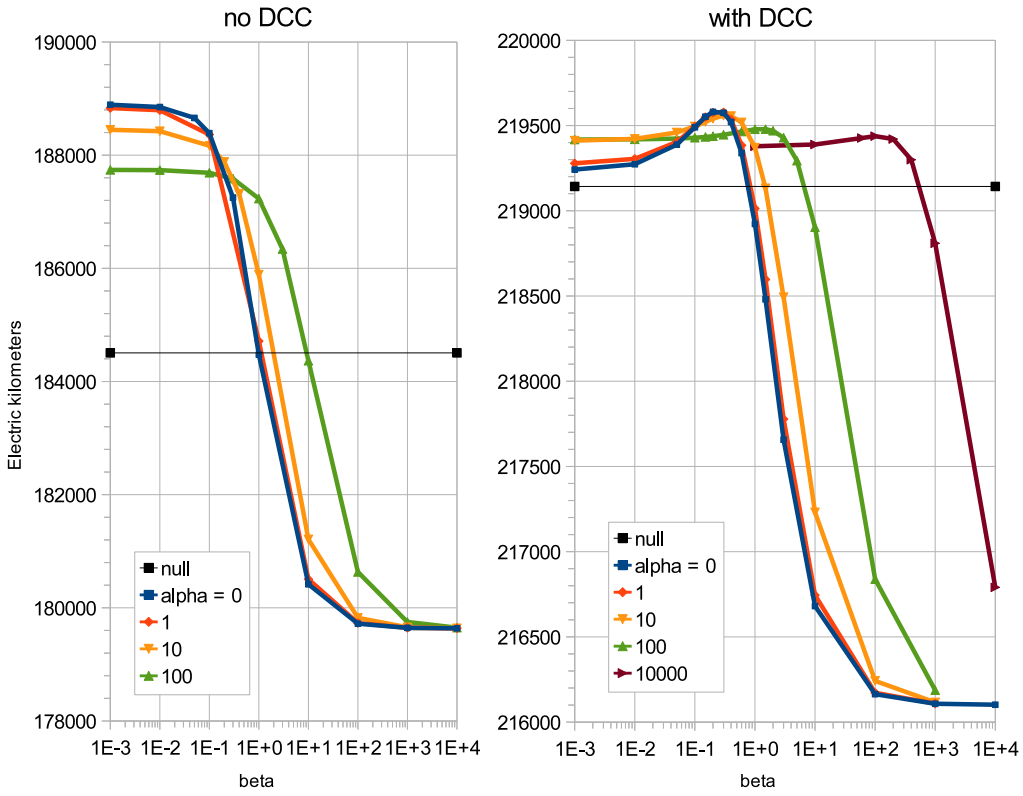

Figure 30: Electric kilometers with different weights of normalized SOC deficit α and capacity β using the linear charging function in (12), with and without DCC. Recharge time is 60 minutes, big factor is 50 %. Small capacity is 2 kWh, big capacity is 6 kWh. The curve labeled "null" shows the amount of electric kilometers obtained using the null-strategy.

the grid. For simplicity, the energy-based approach will be used in this section.

For the simulations, the exact prediction data is obtained by repeating the same simulated day as explained in section 5.1.4. A potential source of information in the real life is the car fleet itself. If the car is sufficiently advanced, it can collect travel data. It can, for example, be able to give the distribution of the total travel distance from workplace to home or the distribution of the stationary time at the workplace. It is possible that the car uses GPS/WLAN and/or time to figure out when it's at the workplace or that the owner will give this information manually. A proposal for obtaining a prediction for the next free distance at the workplace is given in A.4.

5.2.1 Prediction error

Both the stationary time and the next free distance are known exactly from previous simulations, so an error term ε is introduced to represent inaccuracy in the prediction. This makes the stationary time T and next free distance D take the following form:

$$\begin{aligned} T &= \max(T_0 + \varepsilon_T, 0) \\ D &= \max(D_0 + \varepsilon_D, 0) \end{aligned} \tag{13}$$

where T_0 and D_0 are the exactly known stationary time in timesteps and next free distance in kilometers, respectively. The error terms ε_T and ε_D are:

$$\begin{aligned} \varepsilon_T &= \delta\, \sigma_T\, r_T \\ \varepsilon_D &= \delta\, \sigma_D\, r_D \end{aligned} \tag{14}$$

where $\delta \geq 0$, the *prediction error*, is a free parameter to allow for the easy manipulation of the inaccuracy, σ is a constant to represent the standard deviation of the error and r is a normally distributed random number[5] with mean 0 and variance 1. We chose $\sigma_T = 12$, which corresponds to one hour, and $\sigma_D = 5$, corresponding to 5 km.

T and D are updated each timestep so that if we pass the predicted departure timestep, the program will continue assuming that the car will leave during the current timestep, until the car actually leaves the node.

5.2.2 Implementation

Intuitively, the charging function should account for the stationary time, energy and next free distance in the following way:

- If stationary time is small, attempt to increase charging power. If stationary time is large, attempt to decrease charging power.
- If energy is low, attempt to increase charging power. If energy is high, attempt to decrease charging power.

[5] r should be picked from a new random number stream so that it doesn't affect the movement of cars.

- If next free distance is small, attempt to decrease charging power. If next free distance is large, attempt to increase charging power.

If the next free distance D is known exactly i.e. prediction error is zero, the current energy E is redundant as we now know the actual required energy

$$\check{E} = Dc - E \tag{15}$$

where c is the electricity consumption in kWh/km. However, because in reality the next free distance is often *not* known exactly ($\delta > 0$), the term αE should be kept in the argument of the exponent function.

To implement stationary time T and next free distance D, the charging function should take a form where a large $T > 0$ decreases the bandwidth and large $D > 0$ increases the bandwidth:

$$\begin{aligned} z(E,D,2T,...) &< z(E,D,T,...) \\ z(E,2D,T,...) &> z(E,D,T,...) \end{aligned} \tag{16}$$

A function that satisfies (16) is

$$\begin{aligned} z &= \exp(\alpha E)\exp(\beta\check{E})/\exp(\gamma T) \\ &= \exp\left(\alpha E + \beta(Dc - E) - \gamma T\right) \end{aligned} \tag{17}$$

where $\beta, \gamma > 0$ are weight parameters. With this charging function, it is possible to conveniently study the cases where the information about stationary time or next free distance should have no effect on the charging by setting either β or γ to zero. By setting both weights $\beta = \gamma = 0$, this function reduces to the function in (10).

For simplicity, we are going to first study the effect of weight of stationary time γ together with prediction error δ (so that weight of next free distance $\beta = 0$), then the effects of β together with δ (so that $\gamma = 0$) and finally all three together. It is assumed that the weight of energy $\alpha = -1$, because, in most cases, more electric kilometers were gained with small negative values for this parameter.

5.2.3 Effect of stationary time

Simulations were run with five different values for prediction error δ and several values of weight of stationary time γ with weight of energy $\alpha = -1$ and weight of next free distance $\beta = 0$. The results are shown in Figure 31. Increasing the error in stationary time seems to bring the electric kilometer curve asymptotically towards a horizontal line, but with a peak at $\gamma = 0$. With greater precision for the prediction it is possible to achieve greater electric kilometer gains. This also makes it possible to achieve greater losses with negative (counterproductive) values for the weight parameter. Note how all the curves travel through the same point at $\gamma = 0$. This is because the prediction error only has an effect when the prediction is used. Also, note how a global optimum emerges at $\gamma = 0$ when the error increases beyond a certain point. A maximum at $\gamma = 0$ implies that the best approach is to ignore the prediction for stationary time completely. Note that this maximum is not at 0 % NSCI due to weight of energy α being nonzero.

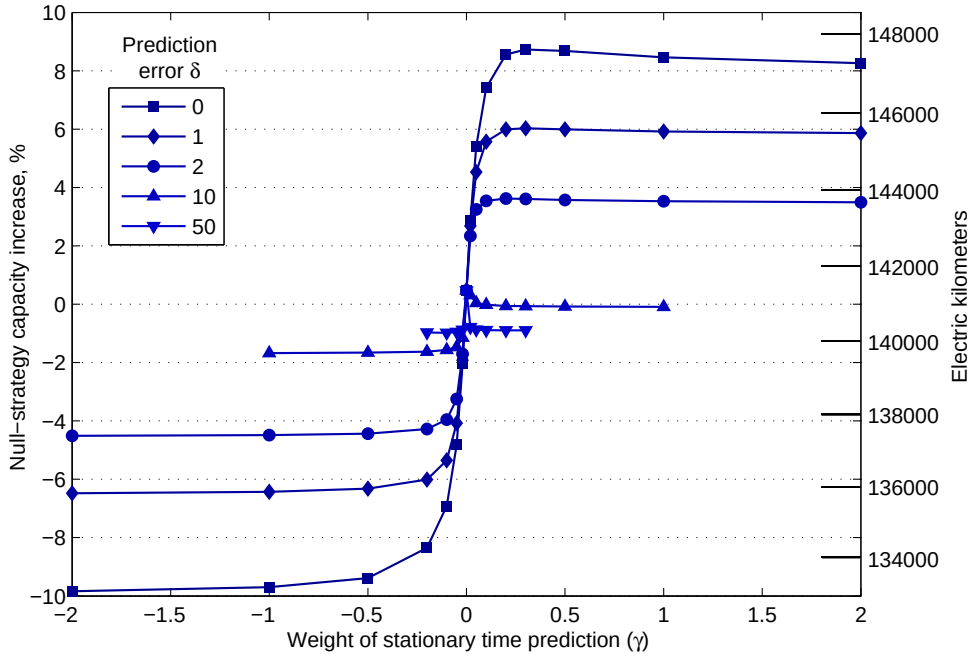

Figure 31: Electric kilometers and NSCI with different weight of stationary time γ and prediction error δ using the charging function in (17). Weight of energy $\alpha = -1$, weight of next free distance prediction $\beta = 0$, recharge time is 60 min, big factor is 0 %. Some data points have been excluded due to corruption from round-off errors.

In order to determine the limit for the error δ beyond which the stationary time prediction is not accurate enough to be useful, a simulation was run with the same parameters as in Figure 24, but with the weight of the prediction γ ranging between $[-0.02, 0.02]$.

According to Figure 32, when the prediction error δ exceeds the value 9, it is best to ignore stationary time and set the weight of the prediction to zero ($\gamma = 0$). This corresponds to having a normally distributed error with standard deviation larger than 9 hours.

To study the effects of weight of stationary time γ in an environment with different battery capacities, a simulation was run with 2 kWh and 6 kWh batteries using big factor 50 %, with and without DCC. The results are shown in Figure 33. It seems that with DCC γ has a smaller effect on the electric kilometer count, possibly due to the decrease in the priority differences as suggested in section 5.1.5.

5.2.4 Effect of next free distance

In order to study the effect of the required energy term $\beta(Dc - E)$ in the charging function exponent, we disable the use of the prediction for stationary time by setting $\gamma = 0$, while keeping the weight of energy at $\alpha = -1$. The simulation was run with different weights β and errors δ.

The results are shown in Figure 34. It is immediately seen that the NSCI curves resemble qualitatively the curves in Figure 31.

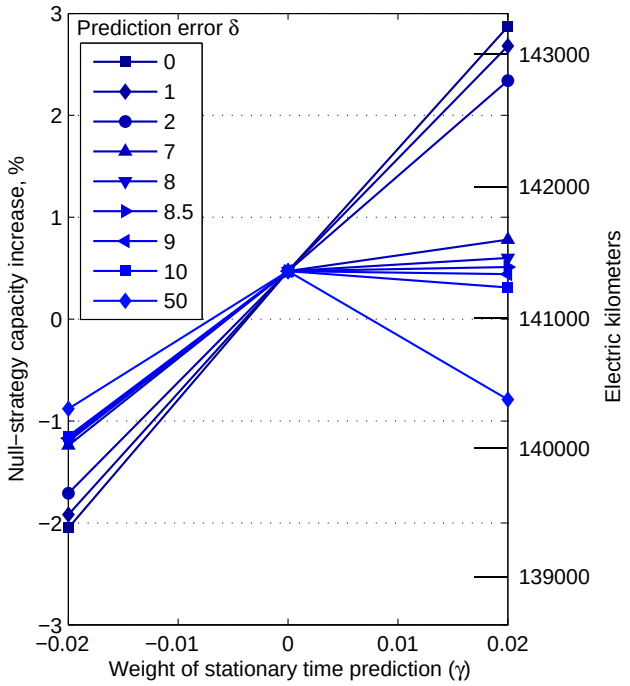

Figure 32: Electric kilometers and NSCI with different weight of stationary time prediction γ and prediction error δ using the charging function in (17).

It is possible to ignore energy E by setting its weight $\alpha = 0$, and thus focus completely on the required energy ($Dc - E$). When there is no error ($\delta = 0$) and the prediction weight β is sufficiently large, setting the weight of energy $\alpha = 0$ increases the electric kilometers, see Figure 35. This is because the amount of energy the car requires is now known exactly. Having the absolute energy term only throws the charging function off. However, when the error is large ($\delta = 10$), having a negative weight of energy α increases the amount of electric kilometers.

At a glance it would seem that these curves also have an optimum at zero prediction weight ($\beta = 0$) when the prediction error gets large enough. However, this is not the case, for the global optimum is on the positive side, at roughly $\beta = 0.02$. In fact, there are two turning points:

1. the prediction for next free distance gets so inaccurate that it is best not to increase β from 0.02.

2. the prediction for next free distance gets so inaccurate that it is best to ignore the next free distance completely by setting $\beta = 0$

The first of these is reached when prediction error $\delta > 9$ (see Figure 36). This corresponds to having an error with the standard deviation larger than 45 km. The global optimum is then located at around $\beta = 0.02$. The second turning point is reached when $\delta > 21$ (see Figure 37). This corresponds to

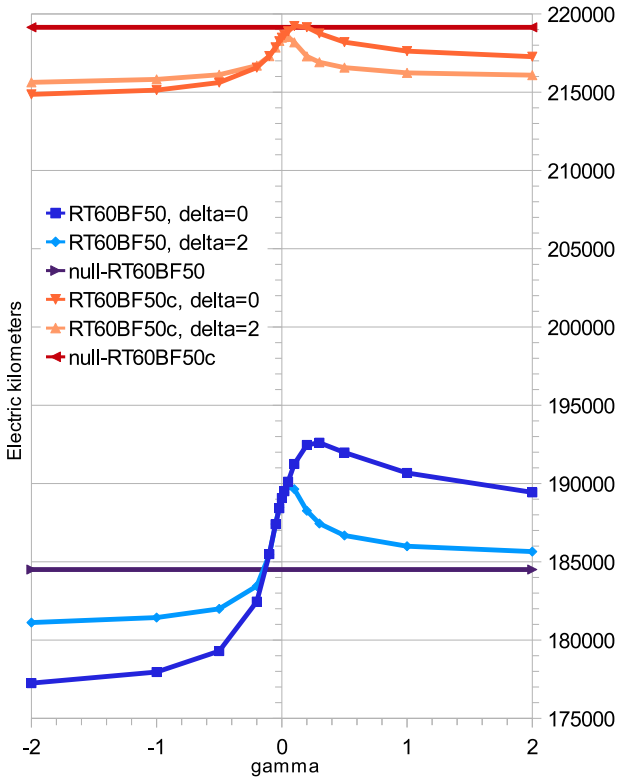

Figure 33: Electric kilometers as a function of weight of stationary time prediction γ using the charging function in (17), with different prediction error δ, with and without DCC. Weight of energy $\alpha = -1$, weight of next free distance $\beta = 0$. For label explanations, see section 5.1.5.

standard deviation larger than 105 km. The global optimum is then shifted to $\beta = 0$, where the prediction is completely ignored.

5.2.5 Using both stationary time and next free distance

It will now be checked how these two different predictions affect when both are enabled simultaneously. For simplicity, we assumed that there was no error in either prediction ($\delta = 0$). If there is no error in the prediction for the required energy, we can set the weight of energy α to zero, as explained in section 5.2.4. The results are shown in Figure 39.

Apparently, the electric kilometer curves converge toward a common value when the absolute value of β is very large. If β is much larger than γ (and α), the prediction for the next free distance dominates the value of the charging function, causing the stationary time prediction to have less effect. Electric kilometers will then decrease, because we are throwing data away by undermining the usefulness of the prediction for the stationary time.

When the weight of stationary time is negative ($\gamma < 0$), it is actually advantageous to undermine the stationary time prediction by setting $|\beta| \gg$

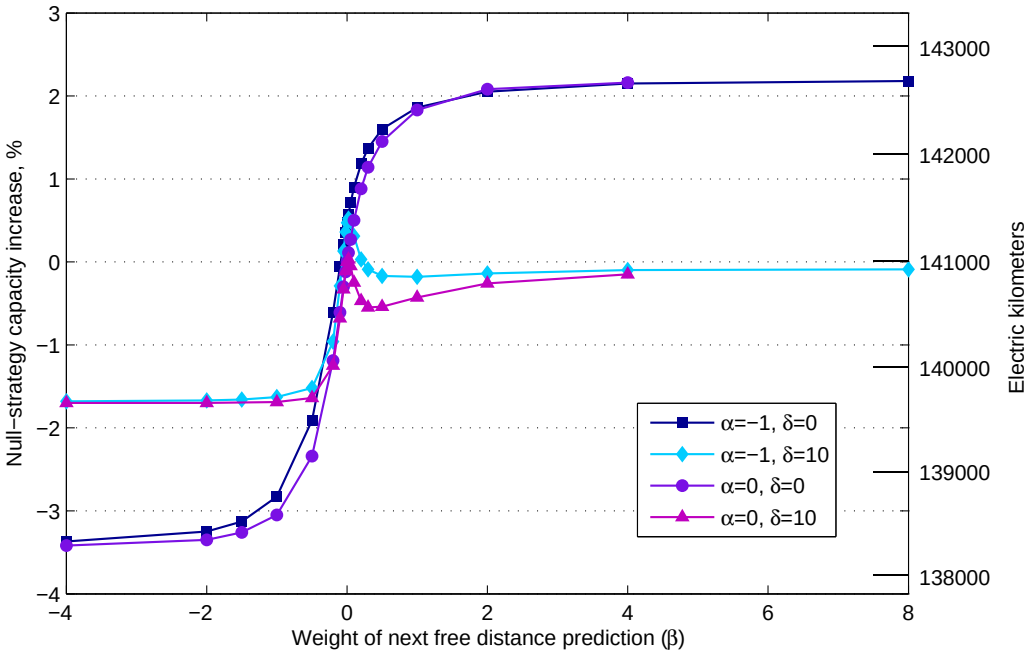

Figure 34: Electric kilometers and NSCI with different weight of next free distance prediction β, weight of energy α and prediction error δ using the charging function in (17). Weight of stationary time prediction $\gamma = 0$, stationary time error multiplier $\sigma_T = 12$, recharge time is 60 min, big factor is 0 %.

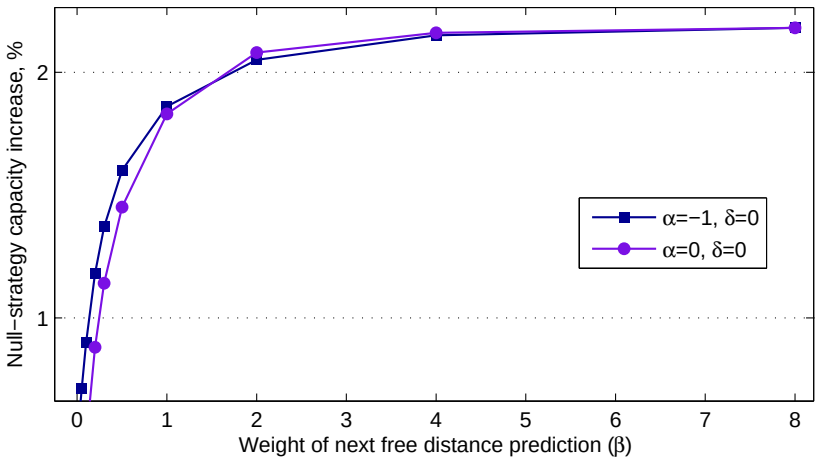

Figure 35: Zoomed-in version of Figure 34.

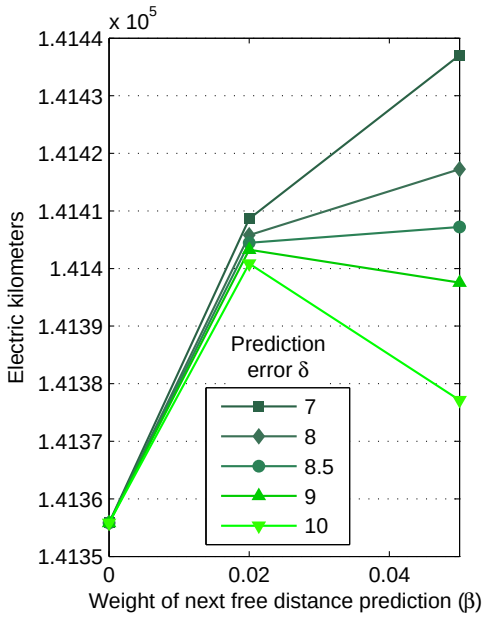

Figure 36: The first turning point. Electric kilometers with different weight of next free distance prediction β and prediction error δ using the charging function in (17). Weight of energy $\alpha = -1$, weight of stationary time prediction $\gamma = 0$, recharge time is 60 min, big factor is 0 %.

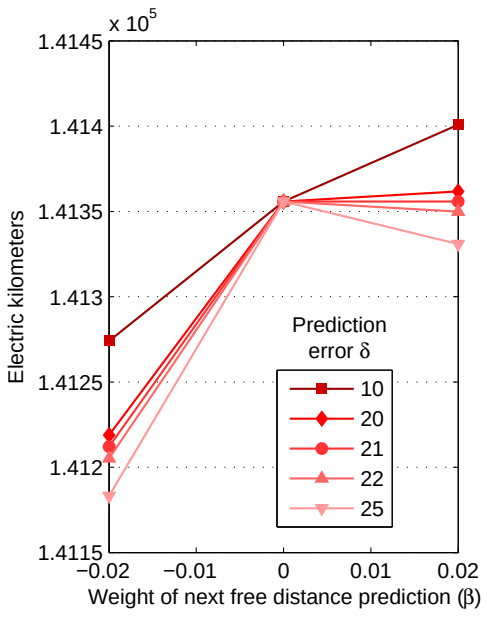

Figure 37: The second turning point. Electric kilometers with different weight of next free distance prediction β and prediction error δ using the charging function in (17). Weight of energy $\alpha = -1$, weight of stationary time prediction $\gamma = 0$, recharge time is 60 min, big factor is 0 %.

γ to obtain more electric kilometers for there is a global minimum at $\beta = 0$. In practice, however, the weight of stationary time should never be less than zero, as this would penalize the cars that will spend less time at the node.

Increasing the weight of next free distance β seems to have a smaller effect than increasing the weight of stationary time γ (see Table 1), which seems to indicate that the prediction for stationary time is more useful than the prediction for the next free distance. This does not imply that we should ignore the latter, because it can increase the electric kilometers. When the prediction error is low, both predictions should be used to maximize utility.

In order to obtain more evidence for the hypothesis that stationary time is more useful than next free distance, the following two strategies were tested:

$$\begin{aligned} z_{\text{NFD}} &= \exp\left(\beta(Dc - E)\right) \\ z_{\text{ST}} &= \exp(-\gamma T) \end{aligned} \tag{18}$$

which are simply the charging function in (17) with the weight of energy α set to zero and the weights of next free distance and stationary time (β and γ, respectively) set to zero alternatively. For additional data, both the capacity and the workplace power factor were increased by 100 % and reduced by 50 %. Thus the simulation was run in a total of nine different

Table 1: Electric kilometer values from Figure 39.

	$\gamma = 0$	$\gamma = 0.5$
$\beta = 0$	140 992	147 025
$\beta = 0.5$	142 119	147 518

scenarios for both charging functions. For simplicity, perfect predictions were assumed ($\delta = 0$). The electric kilometers for different coefficients are shown in Figure 38. "Coefficient" refers to β when using the function z_{NFD} and to γ when using the function z_{ST}. These two cases are labeled in the Figure as "NFD" and "ST", respectively.

It is seen that in eight of the nine scenarios, the greatest amount of electric kilometers were obtained using the prediction for stationary time, assuming optimal value for the coefficient. The scenario with capacity 1 kWh and workplace power factor 0.2 kW is ambiguous due to the electric kilometers reaching the maximum as seen in Figure 16.

5.2.6 Balance between prediction and observed average

When the prediction is very inaccurate, it is reasonable to use the observed average instead in the calculations. But what happens if the prediction is only moderately inaccurate? To study this problem in the stationary time case, the following charging function was experimented with:

$$z = \frac{\hat{y} - E}{Tw + \bar{T}(1-w) + 1} \tag{19}$$

where $\hat{y}$, E and T are the maximum capacity in the system, energy of the battery and stationary time, respectively, and

$$\bar{T} = \max(\bar{L} - t, 0) \tag{20}$$

where $\bar{L}$ is the average work leaving timestep[6] and t is the current timestep. w sets the preference of prediction versus average. If $w = 0$, only the average is used, and if $w = 1$, only the prediction is used.

Null-strategy capacities with different prediction errors and battery capacities are shown in Figure 40. It is seen that with low prediction error, more electric kilometers are gained by setting $w = 1$ i.e. ignoring the average and giving complete focus on the prediction. With large prediction error, we should set $w = 0$, ignoring the prediction and giving the focus on the average. With intermediate prediction error, there is an electric kilometer maximum with $0 < w < 1$. This result is sensible, because accurate predictions (ones with low error) divulge useful information about which car to favor. When the error gets worse, it is possible to safeguard against inaccurate predictions by gravitating the prediction towards the observed average by reducing the value of w. When the error gets too large, the predictions give mostly misinformation. In that case, the predictions should be ignored altogether by setting $w = 0$.

[6] When calculating this average, those cars that do not go to work are simply ignored.

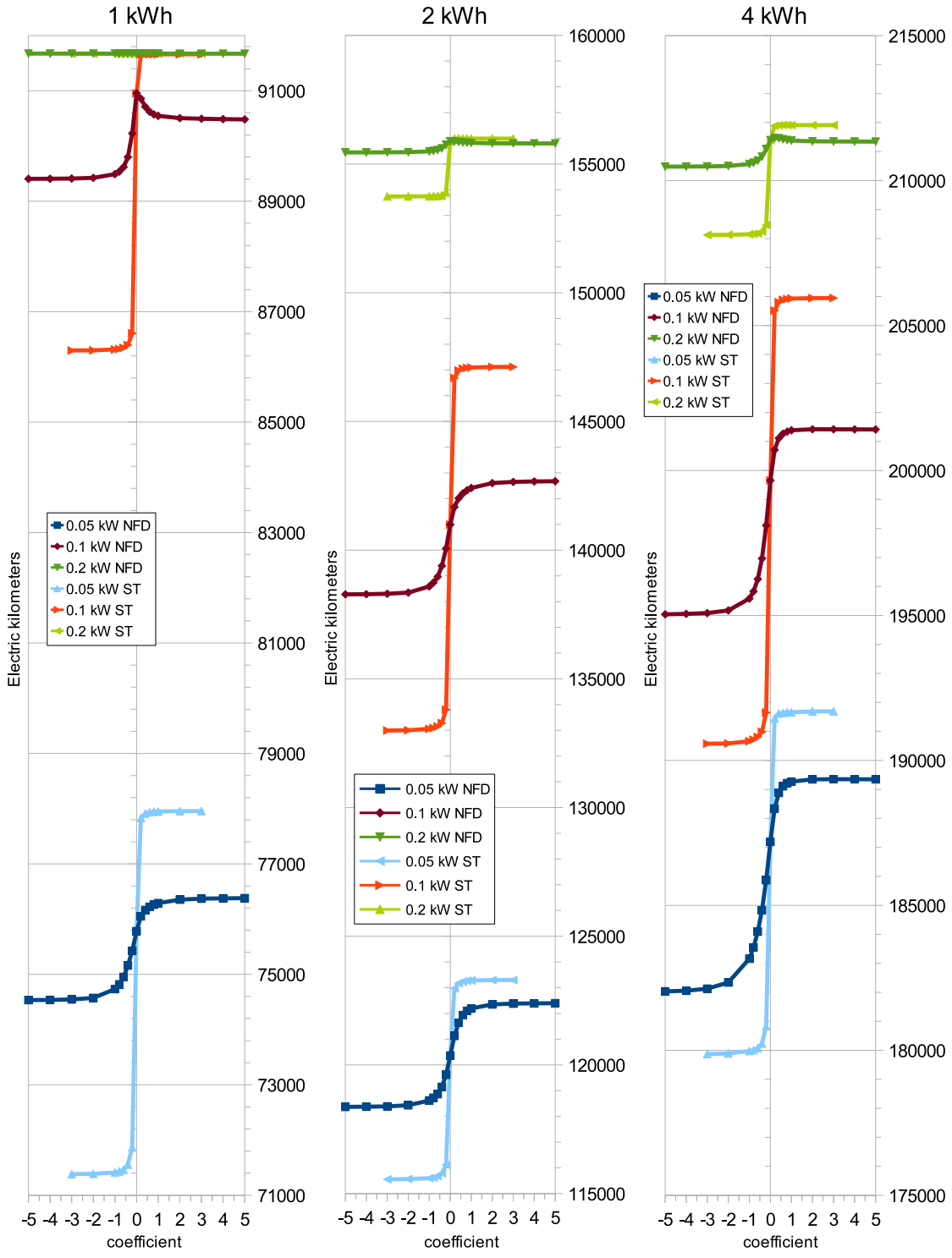

Figure 38: Electric kilometers with different coefficients of prediction using the charging functions in (18), with three different battery capacities (1 kWh, 2 kWh and 4 kWh) and three different workplace power factors (0.05 kW, 0.1 kW and 0.2 kW per inhabitant. For label explanations, see section 5.2.5.

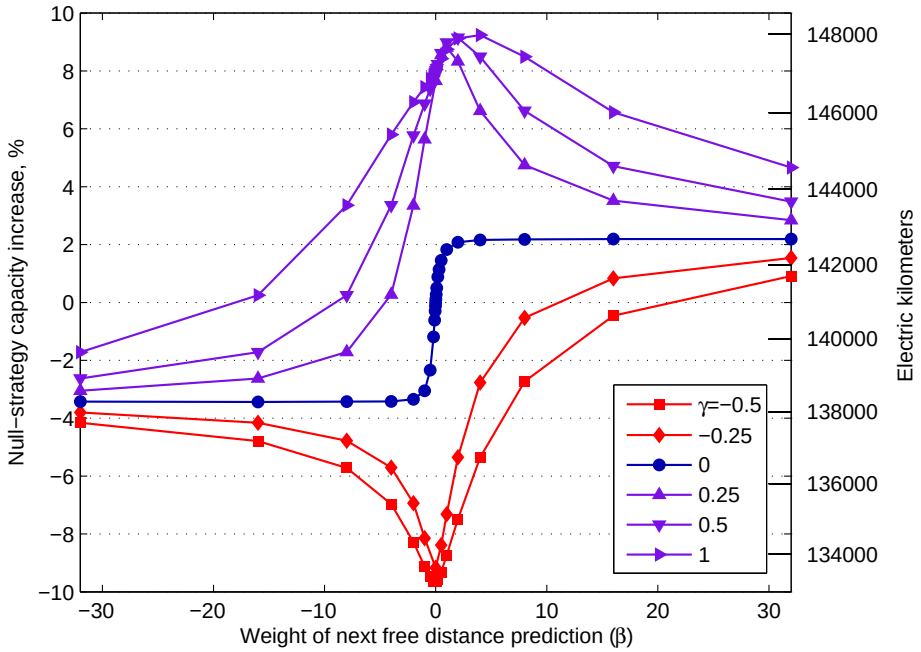

Figure 39: Electric kilometers with different weight of next free distance prediction β and weight of stationary time prediction γ using the charging function in (17), with perfect prediction accuracy ($\delta = 0$). Weight of energy $\alpha = 0$, recharge time is 60 min, big factor is 0 %.

Note how with capacity of 1 kWh, the null-strategy capacity starts *below* 1 kWh with the prediction ignored ($w = 0$), whereas with larger capacities the null-strategy capacity starts *above* the current capacity. It seems that the energy term $(\hat{y} - E)$ throws off the strategy with very low capacities, because without this term, i.e. using the charging function

$$z_- = \frac{1}{Tw + \bar{T}(1-w) + 1} \tag{21}$$

the null-strategy capacity at $w = 0$ is larger than 1 kWh, as seen in Figure 41. All the lines in this picture start at exactly 1 kWh null-strategy capacity, because the average work leaving timestep $\bar{L}$ is same for all cars and thus all cars receive the same weight, which, by definition, corresponds to the null-strategy. There is a slight decay in NSCI near $w = 1$ in the cases where the error is low, $\delta = 0$ and $\delta = 2$. This is presumably due to off-by-one errors when calculating the stationary time from the location data.

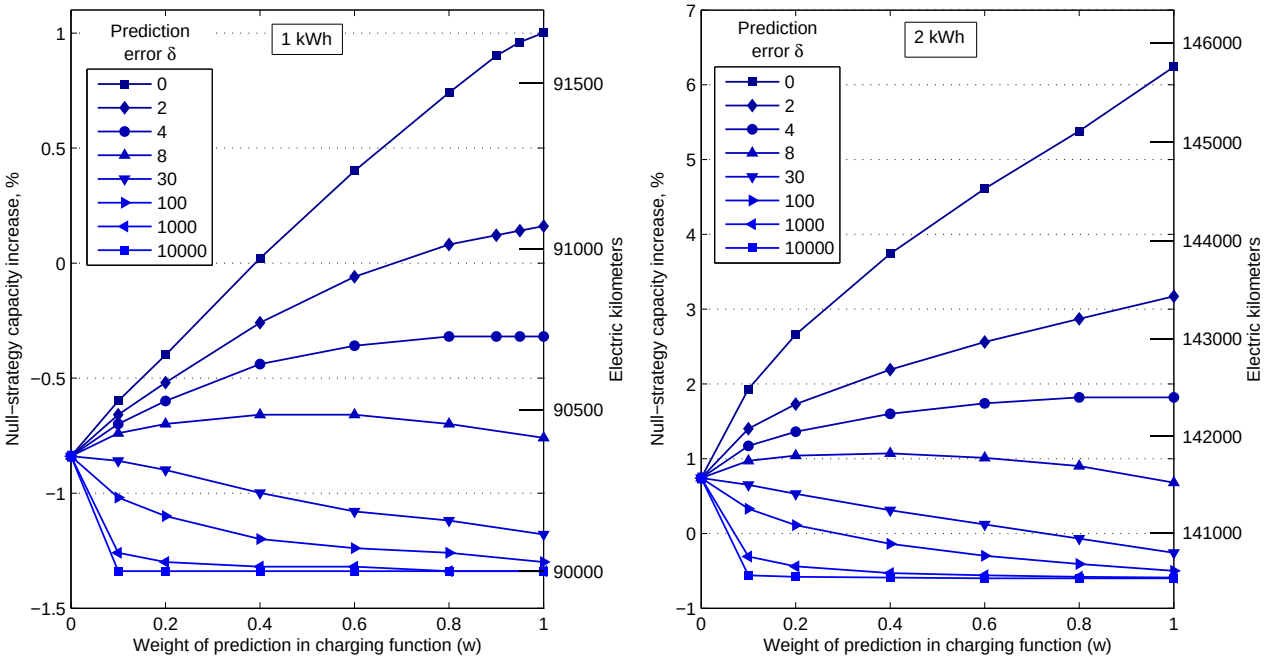

(a) 1 kWh **(b)** 2 kWh

(c) 5 kWh **(d)** 10 kWh

Figure 40: Electric kilometers and NSCI with different parameter w and prediction error δ using the charging function in (19), with four different battery capacities (1 kWh, 2 kWh, 5 kWh and 10 kWh).

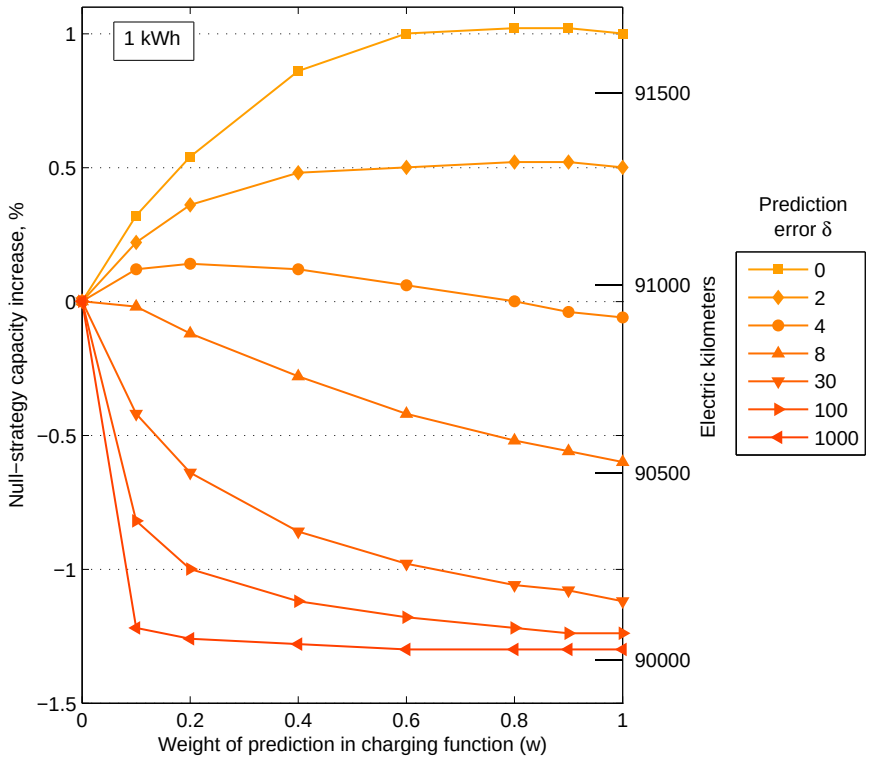

Figure 41: Electric kilometers and NSCI with different parameter w and prediction error δ using the charging function in (21) with the capacity being 1 kWh.

5.3 Effect of workplace charging strategies

To conclude the workplace strategy discussion, the utility gained from the smart workplace charging is now estimated. The strategy in Equation (17) will be used, as this strategy seems the most promising. The workplace power factor is kept at 0.1 kW.

Because the next free distance prediction does not seem to be as important as the stationary time prediction, we set its weight $\beta = 0$. The weight of stationary time γ is set to 1, for this seems appealing according to Figure 31. The charging function then takes the form

$$z = \exp(\alpha E - T) \tag{22}$$

For simplicity, it is assumed that there is no error in the stationary time prediction.

The electric kilometers with different capacities (big factor 0 %) and weight of energy α are shown in Figure 42. The electric kilometers obtained using the null-strategy, labeled "null", and those obtained by removing the power limitation at workplace nodes [7], labeled "full", are also plotted in this figure. Apparently the capacity of the simulated cars is significant when determining the effectiveness of any strategy. This is seen in the difference of full kilometers and the null kilometers with each capacity. With low capacities, the strategy has no room to operate. With high capacities, the strategy does not affect the electric kilometers [8] as the cars will have enough energy for the home trip regardless.

The difference of full and null kilometers are plotted, along with the "strategy" (labeled "strat") kilometers i.e. kilometers obtained with the power limitation, but using the strategy in (22) with optimized weight of energy α, in Figure 43. Their ratio and the corresponding NSCI values are also shown. Full kilometers minus null kilometers ("full-null") peaks with capacity 2.5 kWh. With this capacity, the charging strategy has the most potential. Strategy kilometers minus null kilometers ("strat-null") in both figures shows how much utility is gained from the charging function. It is seen that, with this charging function, the most utility, 9180 km, is gained with capacity 3 kWh, corresponding to 11 % NSCI.

[7] This gives an upper bound for the electric kilometers obtained using *any* strategy. However, this is not the lowest upper bound.

[8] Again assuming that there is only recharging and no discharging.

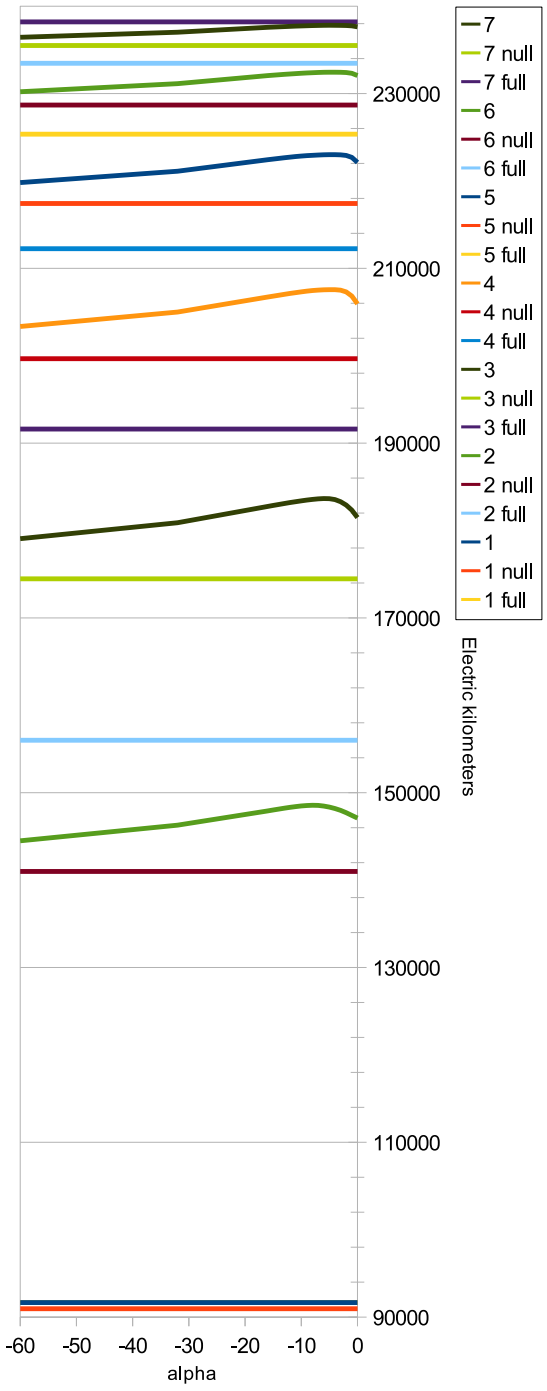

Figure 42: Electric kilometers with different weight of energy α and capacities 1-7 kWh using the charging function in (22). Recharge time is 60 min, big factor is 0 %. For label explanations, see section 5.3.

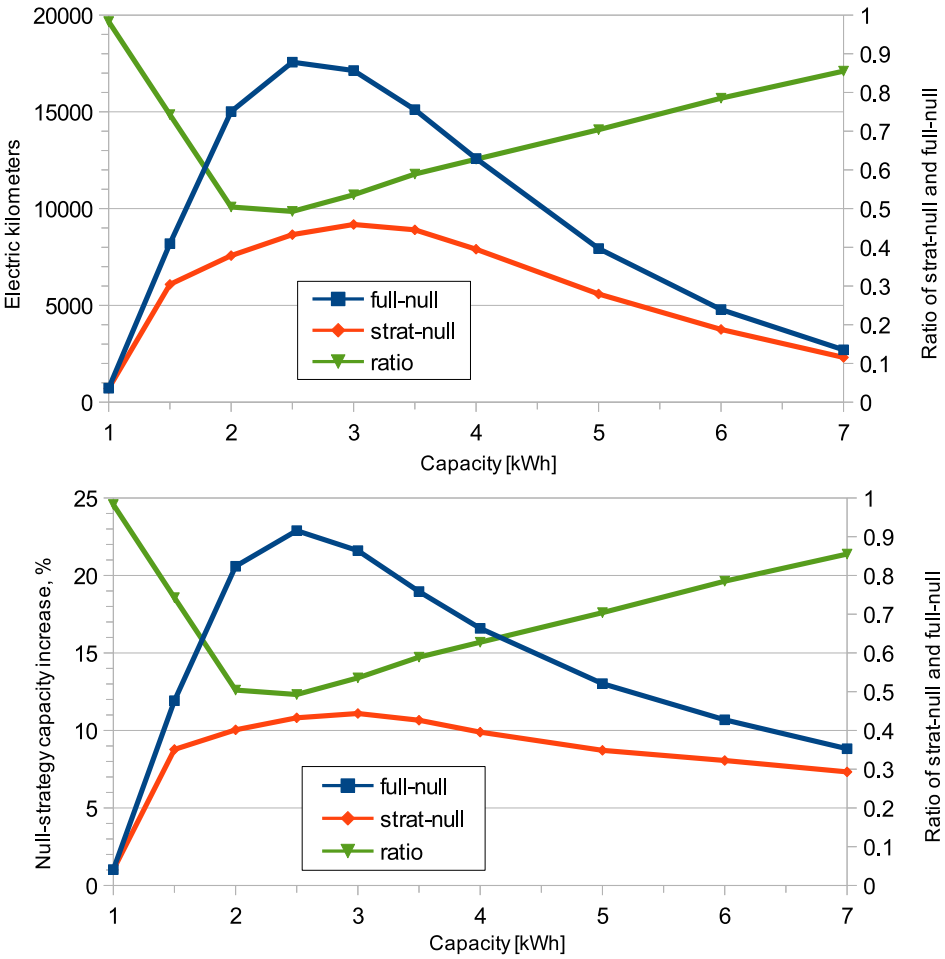

Figure 43: Electric kilometer differences and NSCI extracted from Figure 42. For label explanations, see section 5.3.

6 Home recharging

In this section a method for generating nearly arbitrary charging load profiles is introduced. This method is used to fill the night-time consumption slump in a near-optimal way with a sine-shaped load profile. This sine-shaped load profile is also used to calculate an estimate on how much the standard deviation of power consumption can be reduced by the home recharging on annual scale, with different traffic electrification percentages.

6.1 Weighted random recharging, WRR

Our ultimate goal is to reduce the standard deviation of power by filling the night slump in the base electric power consumption (see Figure 45) using the recharging load of PHEVs. The method used to achieve this is called *weighted random recharging* or WRR.

The principal idea behind WRR is that each car may recharge its battery with its maximum supported power, but the timeframe of recharging, or *recharging interval*, is obtained by sampling a certain distribution. It would be sensible to design this distribution so that it causes the total recharging power profile to fit the night slump as well as possible.

6.1.1 Time intervals

The simulated day is divided into two sections, *daytime* and *night-time*. During the daytime, the charging function is used normally as in section 5. During the night-time, all recharging is forbidden except during the personal recharging interval given by the distribution sample. Night-time is defined as the time interval between timesteps $t_{\mathrm{NS}} = 175$ (night-time start) and $t_{\mathrm{NE}} = 73$ (night-time end)[9]. It is assumed that during night-time the maximum power supported by each home node is infinite.

When a car arrives home with energy deficit D (in kilowatt-hours), it is given its recharging interval midpoint. When calculating the recharging interval, it is assumed that the car is no longer driven for the rest of the day i.e. D remains constant until the recharging interval is reached. If the midpoint is timestep t_{mid}, the recharging interval is defined as $[t_{\mathrm{start}}, t_{\mathrm{end}}]$, where

$$\begin{aligned} t_{\mathrm{start}} &:= \mathrm{floor}\left[t_{\mathrm{mid}} - \frac{D}{2P}\frac{3600}{dt}\right] \\ t_{\mathrm{end}} &:= \mathrm{ceil}\left[t_{\mathrm{mid}} + \frac{D}{2P}\frac{3600}{dt}\right] \end{aligned} \tag{23}$$

where P is the maximum charging power supported by the battery in kilowatts, dt is the length of the timestep in seconds and floor and ceil are round-down and round-up operators, respectively. It may be that the home arrival timestep is greater than t_{start}. If this happens, the car is simply not fully recharged that night.

[9] Night-time end is smaller than night-time start because the simulation jumps back to timestep 1 when timestep 288 ends.

This assigns an energy "block" of roughly size $P \times (t_{\text{end}} - t_{\text{start}})$ for each car[10]. These blocks are then used to fill the nighttime power consumption slump. Because the electricity consumption slump resembles a sine curve, we are going to obtain the midpoints from a sine-shaped distribution. For details, see section A.2.

6.1.2 Obtaining midpoints

The samples r from the sine-shaped distribution have mean zero and variance of roughly 0.047. In order to convert these samples to midpoints, the midpoint of the resulting distribution, the *peak position* t_{PP} is added with multiplier σ_{P}:

$$t_{\text{mid}} := t_{\text{PP}} + r\sigma_{\text{P}} \tag{24}$$

Using this method, a roughly sine-shaped power consumption curve is obtained as seen in Figure 44. Because the battery energy deficits vary, the curve has both a head and a tail. Note how there is a small amount of home recharging before all recharging is suddenly stopped when the WRR interval is reached.

6.1.3 Optimizing parameters

The parameters that form the WRR consumption profile are now optimized so that it would fit the night consumption pit in near-optimal way. The optimal parameters are defined so that they, when used in the WRR, minimize the standard deviation of the total power consumption profile. We assume that there are 240 000 cars.

The optimal position $\bar{t}_1$ for the peak is searched first with $\sigma_{\text{P}} = 50$. We then search for the optimal multiplier $\bar{\sigma}_1$ with $t_{\text{PP}} = \bar{t}_1$ using the precision of $\Delta\bar{\sigma}_{\text{P}} = 10$ and then optimize t_{PP} once more with $\sigma_{\text{P}} = \bar{\sigma}_1$[11]. After this the global optimum should be sufficiently close.

The first sub-optimization yielded $\bar{t}_1 = 14$ (see Figures 46 and 47), the second $\bar{\sigma}_1 = 110$ and the final $\bar{t}_2 = 7$, making the near-optimal parameters $t_{\text{PP}} = 7$ and $\sigma_{\text{P}} = 110$. Figure 49 shows how the near-optimized WRR fills the consumption pit. Figure 48 shows how standard deviation is decreased when PHEV recharging power is added to the base consumption profile.

6.2 Reducing standard deviation of electric power consumption on annual scale

The total amount of kilometers driven by car[12] in Finland in 2010 was 46.2 billion [25]. This is around 127 million kilometers per day on average. If those kilometers were driven using electricity, the daily electricity consumption would increase by 25.3 GWh on average (assuming electricity

[10] The block size may vary if the car is driven after it arrives home or if it receives a bad midpoint.

[11] This is the one-at-a-time coordinate-wise optimization method.

[12] Excluding lorries, vans and buses.

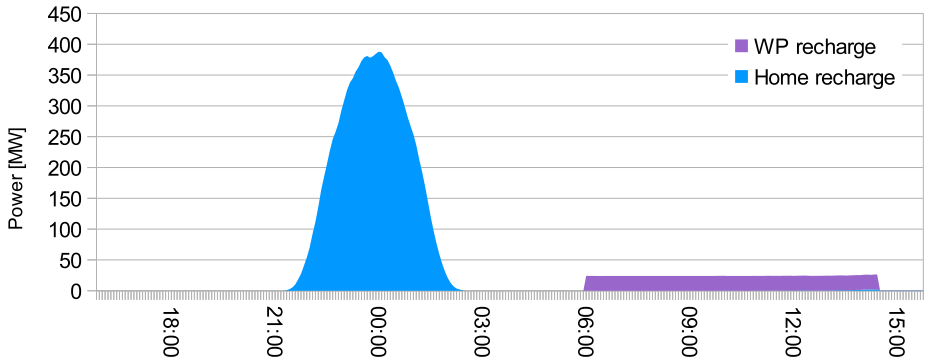

Figure 44: Recharging profile of 20 000 cars scaled to 240 000. Workplace power factor is 0.1 kW, recharging time is 60 min. Battery capacity is 7 kWh. Multiplier σ_{P} = 50, peak position t_{PP}= 288, night-time start t_{NS} = 175, night-time end t_{NE} = 361. r is picked from a sine-shaped distribution.

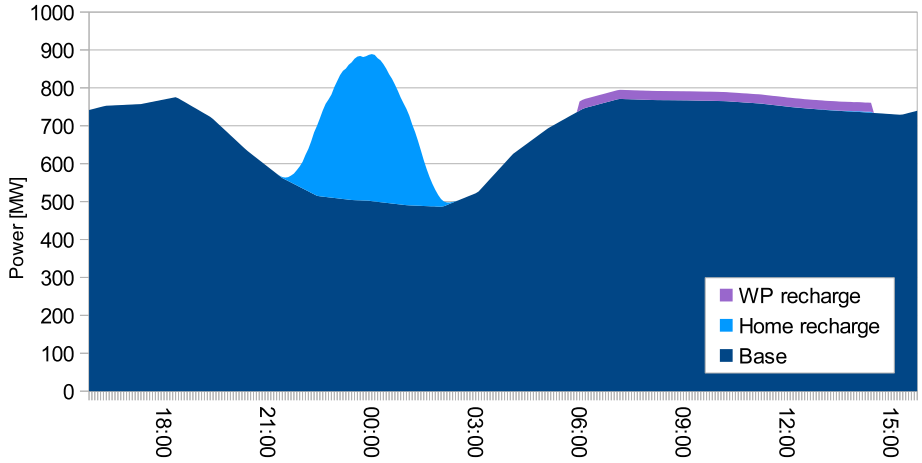

Figure 45: Same as Figure 44, but with base electricity consumption added.

consumption of 200 Wh/km). It is now checked how this additional consumption could decrease the yearly standard deviation of power. The sine-shaped profile in Figure 44 (referred to from now on as *recharging profile*) is scaled so that its integral with respect to time (i.e. energy) equals $(E \times p/100)$, where E is the aforementioned 25.3 GWh and p is the percentage of those kilometers driven using electricity, or the *electrification percentage*.

For simplicity, it is assumed that each day the integral of the recharging profile (the total amount of energy recharged) remains the same. It is also assumed that the position of the recharging profile can be chosen freely between 16:00 the current day and 16:00 the next day, regardless of the population of the home nodes. Also, in this section, 1-minute timesteps are used in place of the 5-minute timesteps used previously.

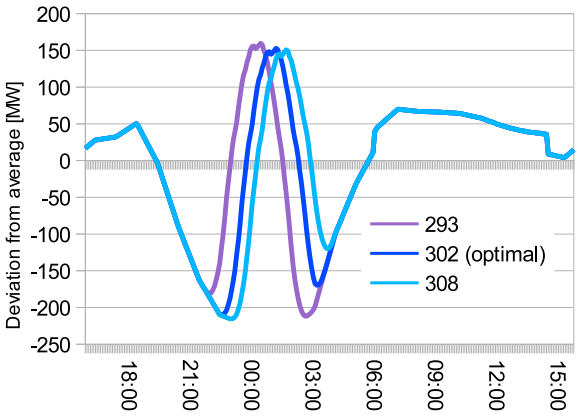

Figure 46: Searching for the optimal peak position. Deviation from the average power consumption as a function of time with different peak positions.

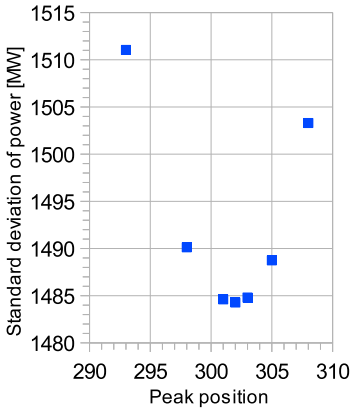

Figure 47: Searching for the optimal peak position. Standard deviation of total power with different peak positions.

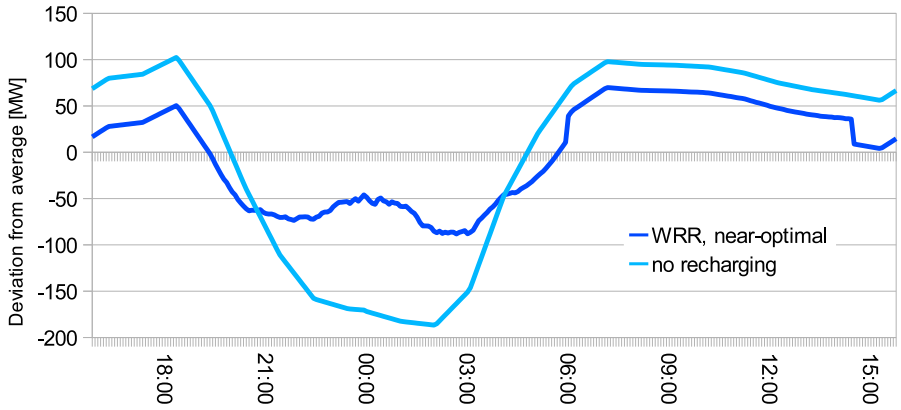

Figure 48: Deviation from average total power. Comparing base consumption profile (no recharging) and base consumption profile with the near-optimal WRR profile added.

6.2.1 Optimization

Two different cases will be studied. In the first one, we search for the year-optimal full width at half maximum (FWHM) and peak position for the recharging profile. These same parameters are used each night to place the recharging profile into the night slump, which means that on some nights the recharging profile may be badly shaped with respect to the base load. This case is called the *whole-year-at-once*-case (WY1).

Day-optimal FWHM and peak position for the recharging profile are searched in the second case. The optimization is thus carried out each simulated day, reducing the number of occasions where the recharging profile is badly shaped for the night slump. This case is called the *each-day-*

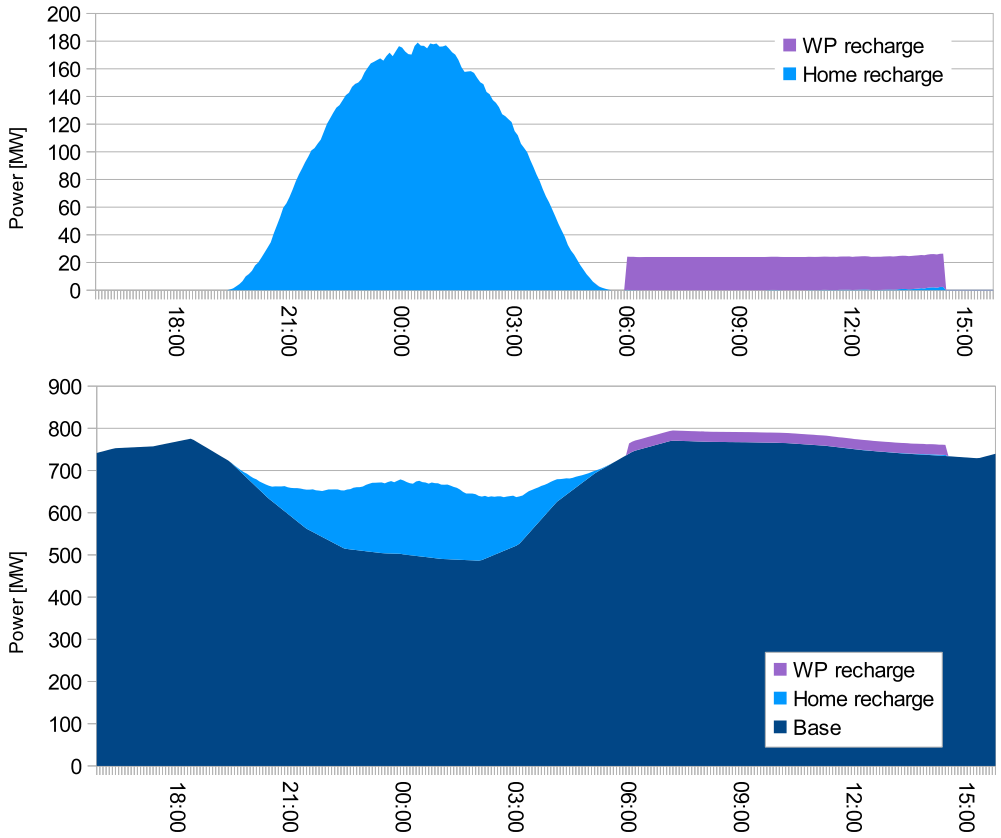

Figure 49: Near-optimal WRR consumption profile, with and without base consumption.

separately-case (EDS). When searching for the optimal FWHM, the profile is manipulated in such a way that the operation does not change the area (energy). For more details on the optimization in the EDS case, see section A.3.

Working day is defined here as as a day that is not Saturday or Sunday. In 2010, there were 261 working days. In this optimization, only working days are considered. This implies that, in the evaluation of the objective function, the standard deviation of power, all days other than working days are skipped. Additionally, the first working day (Friday, first day of January) is skipped in order to simplify the calculations.

6.2.2 Results

The resulting yearly standard deviation with respect to p is shown in Figure 50 for both cases. As expected, when optimizing the parameters for each day separately, a lower standard deviation for the total power can be reached. It is also seen that there is an optimal value ($p = 39$ in the EDS case) beyond which the added electrification of traffic no longer lowers the

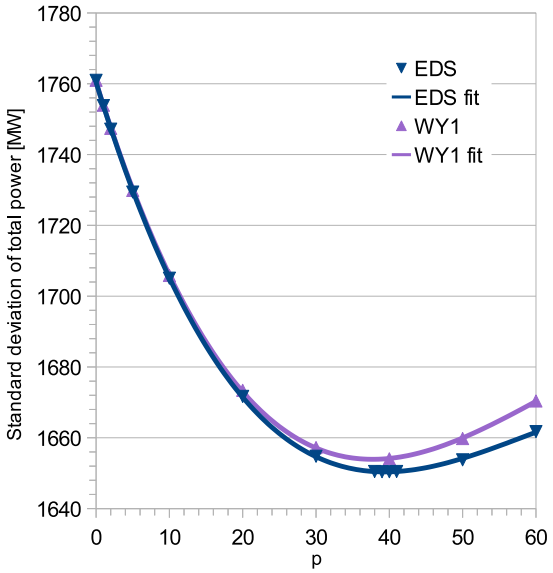

Figure 50: Standard deviation of total power over the whole year with different electrification percentages p in both optimization methods EDS (each day separately) and WY1 (whole year at once). Also showing the cubic polynomial fits to the data.

standard deviation, but *increases* it. This is due to the recharging load overflowing from the night slump. Using this optimal value for p gives a decrease of 6.3 % in the yearly standard deviation and a decrease of 61 % in the mean of daily standard deviation. A third-degree polynomial, shown in the figure as a continuous line, was fitted to both of these data point sets.

The average of optimal time shift and FWHM for both cases are shown in Figures 52 and 53. The first 10 working days with near-optimal recharging added in both cases are shown in Figures 54 and 55. A histogram of the amount of days with a certain standard deviation of power in the near-optimal EDS case is shown in Figure 51. Note how the average of optimal time shift curve in the WY1-case is intermittent unlike the EDS-curve. This is because the WY1-case gives the same parameters for each day, preventing the averaging from smoothing out the curve.

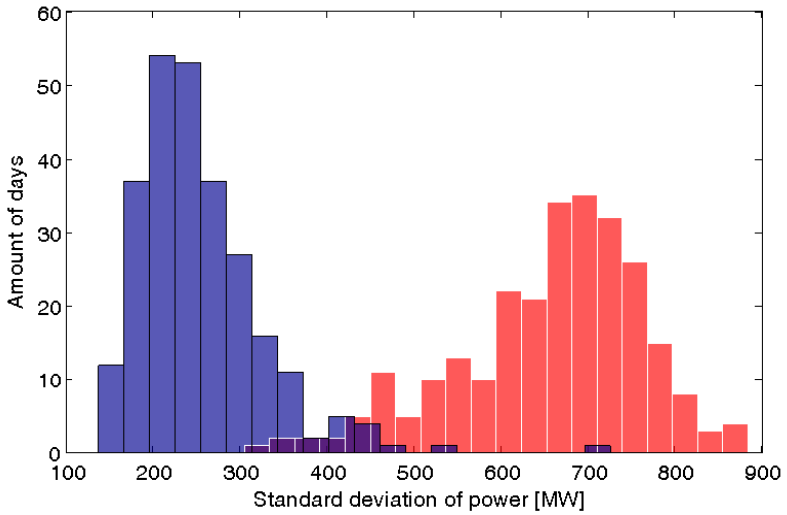

Figure 51: Histogram of the amount of days with a certain standard deviation of power with electrification percentage $p = 39$ and near-optimal recharging profiles in the EDS (each day separately) case before adding PHEV load (red) and after adding PHEV load (blue).

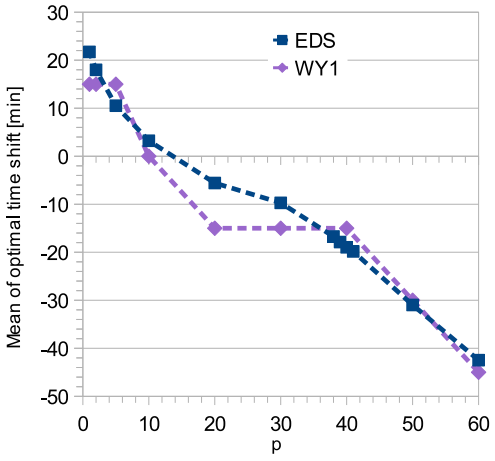

Figure 52: Average of optimal time shift with different electrification percentages p.

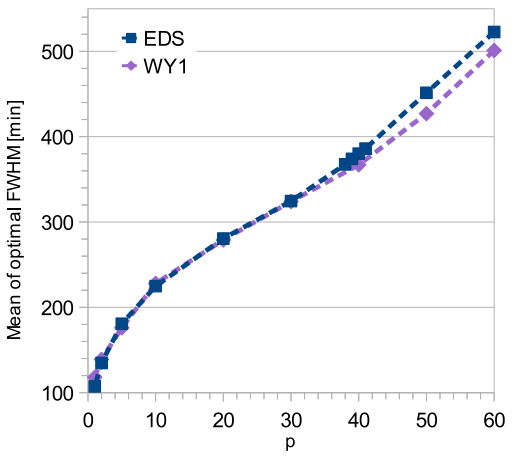

Figure 53: Average of optimal FWHM with different electrification percentages p.

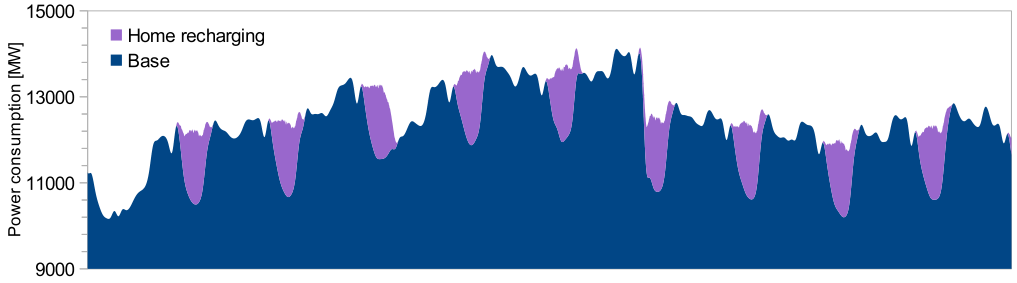

Figure 54: Power consumption on the first 10 working days with electrification percentage $p = 39$ and near-optimal recharging profiles in the WY1 (whole year at once) case.

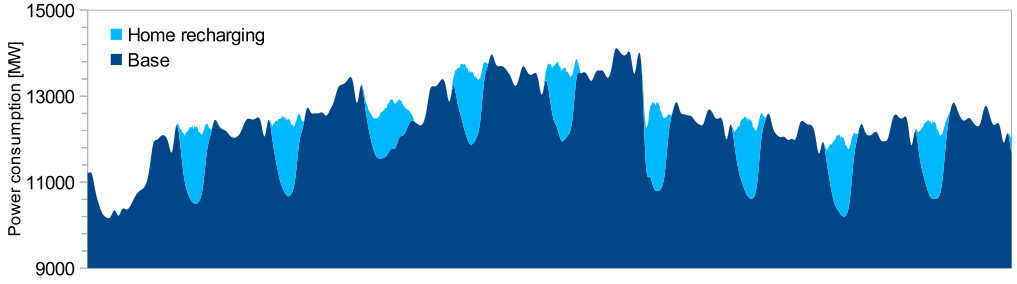

Figure 55: Power consumption on the first 10 working days with electrification percentage $p = 39$ and near-optimal recharging profiles EDS (each day separately) case.

7 Conclusions

In this thesis a model for simulating the movement and charging of PHEVs was used in order to study smart charging. Smart charging was modelled using a charging function that allocates the available power to the connected vehicles. Our results are as follows.

In the case where we use non-predictive charging strategies, if there is no distance-capacity correlation (DCC), it seems that a good strategy is to favor the low-SOC cars instead of the high-SOC cars. This favoring can sometimes be excessive, however, as there may be a global maximum for the electric kilometers using a finite value of the favoring coefficient. This can be seen in Figure 21, with the favoring coefficient being the coefficient of SOC, α. Also with no DCC, low-capacity cars should be favored over high-capacity cars, as seen in Figure 20.

When DCC is enabled, the effectiveness of the strategies diminished to the point where it might actually be advantageous to use the null-strategy (no strategy at all). It seems that enabling DCC provides enough intelligence to make our strategies redundant.

In the case where we use predictive strategies, if the prediction accuracy for the next free distance is insufficient, it is best to include the absolute energy term in the charging function. With accurate predictions, the absolute energy term should be dropped, as seen in Figure 35. This result supports the intuition that it is more important to know the energy that is needed for the return trip than the amount of energy stored in the battery.

It seems that the prediction for the stationary time is more useful than the prediction for the next free distance, see Figure 38. However, for maximal utility gain, both should be used when the predictions are sufficiently accurate.

It is possible to safeguard against the utility loss caused by inaccurate predictions by taking a linear combination of the prediction and the observed average, as seen in Figure 40.

The effectiveness of any strategy is linked to the battery capacity, see Figure 43. With capacity of 3 kWh, recharging power at workplace nodes limited to 0.1 kW per inhabitant and using the charging function in (22), it is possible to gain 9180 more electric kilometers compared to the null-strategy, or 918 m per simulated car. The same amount of kilometers could be gained by using the null-strategy, but increasing the capacity by 11 %, to 3.33 kWh.

It was learned that the weighted random recharging (WRR) method can be used to reduce the daily standard deviation of power consumption, assuming a sufficient amount of vehicles. In the case where the position of the WRR recharging profile was optimized separately each day (EDS-case), we saw that the greatest reduction in the standard deviation was obtained with the traffic electrification of 39 %, as seen in Figure 50. This reduction was 6.3 % for the whole year, while the mean of the daily reduction was 61 %.

During the course of making this thesis, several ideas for future work and improvements were identified. These are explained in the following.

In this study only analytical charging functions were used. However, we could use a table form for the charging function instead. This function

could be optimized using machine learning and evolutionary optimization algorithms.

Our control functions were chosen so that the node populations versus time would look sensible. The control functions could be improved by obtaining real-life data and then tuning the parameters until we get a satisfactory match between simulation and reality.

The fluctuations on the price of electricity were not modelled. This could be implemented simply by modifying the power limitations according to the price. For example, if the price of electricity doubles in some area of our node network, it could halve the power factor at the affected nodes.

The prediction model used could be made more sophisticated. For example, when the work leaving timestep for a car was passed, the program continued to assume that the car would leave the node for all the subsequent timesteps. Instead, this prediction could be flagged as an inaccurate one and some other charging function for the cars that have inaccurate predictions could be used.

Only 1-2 consecutive days and working days were simulated. We could develop control functions for weekends and simulate longer time periods, e.g. a single week to obtain more information and insight.

This model was used to simulate PHEVs and not EVs. If we want to model EV traffic and charging, it is required to take the SOC into account when deciding the next destination, for otherwise the car would run out of electricity during the trip. This would make obtaining predictions more difficult due to feedback issues. A model for traffic congestion could also be included.

Accounting for the correlation between battery capacity and travelled kilometers was greatly simplified in this thesis. There were only two cases, DCC enabled and DCC disabled. If the correlation is used in a continuous way instead, it would be possible to calculate how much of the utility obtained using a given strategy could be replicated by introducing a certain amount of correlation using the null-strategy. Also, the amount of available capacities could be increased, as only a maximum of two different capacities were used at any time.

Shopping and hobby nodes were assumed to offer no recharging service. Recharging could be allowed at these nodes or some of these nodes in order to see if the strategies are affected or if additional strategies are needed for different types of nodes.

Due to the massive amount of input parameters for the simulation combined with the curse of dimensionality, it was necessary to leave a great many interesting parameter combinations unstudied. There is a lot of room for additional experimentation.

A Appendix

A.1 Generating the fed-up factor f

We would like the fed-up factor distribution to resemble a normal distribution, but it is not possible use the normal distribution as it is, because f needs to be in the interval $[0,1]$. This problem is solved by using the following method:

1. Generate r, a normally distributed random number with mean 0.5 and variance 0.04.

2. If $r < 0$ or $r > 1$, go to step 1. Else, finish with $f \leftarrow r$.

A histogram of 100 000 samples from this algorithm is shown in Figure 56.

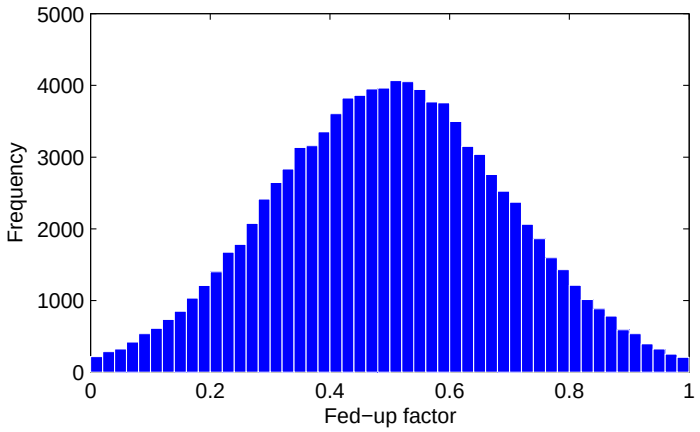

Figure 56: Histogram of 100 000 samples from the fed-up factor generating algorithm.

A.2 Random number from a sine distribution

The inverse-cumulative distribution function method of generating random numbers is used here.

1. Generate x, a uniformly distributed random number between 0 and 1.

2. Calculate

$$r = \arccos(1-2x)/\pi - 1/2 \tag{25}$$

Numbers r_i generated this way follow a sine-shaped distribution, as seen in Figure 57.

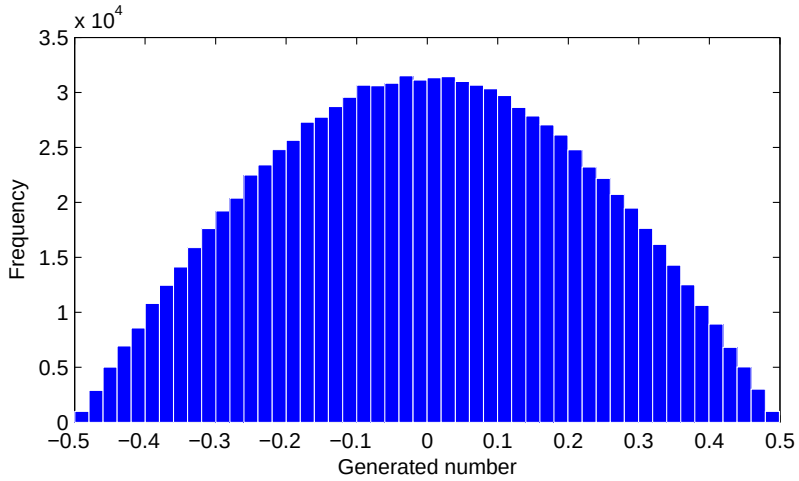

Figure 57: Histogram of 1 000 000 samples from the sine-distributed random number generating algorithm.

A.3 EDS optimization algorithm

The algorithm in the EDS-case works as follows:

1. $d \leftarrow 2$
2. $t \leftarrow$ timestep that corresponds to 4:00 of working day d
3. Find optimal $\theta = \bar{\theta}$ and $\Delta t = \bar{\Delta t}$ for the recharging profile so that the standard deviation in total power (base + recharging) in the timestep interval $\{t-720, t+720\}$ is minimized[13]. The search area is $\{0.1, 2\}$ for θ and $\{-150, 150\}$ for Δt. The search resolution is 0.02 for θ and 15 for Δt.
4. Add the optimal recharging profile to the base power consumption so that its peak position is $t + \Delta t$.
5. $d \leftarrow d + 1$. If $d = 262$, end. Else, go to step 2.

A.4 Approximating the next free distance at workplace

The car's current SOC can be used to extract an approximation for the minimum of the next free distance. This can be done under the following assumptions:

- Car has just arrived to its workplace.
- Car has been fully recharged at home during the night.
- Car has taken the shortest route to its workplace and has not made any stops on the way.
- Recharging is possible only at home and at the workplace.

[13] We are using 1-minute timesteps, so that 720 timesteps correspond to 12 hours.

If the car's current SOC in kilowatt-hours is SOC and its maximum SOC is SOC_{max}, it is possible to calculate the energy it has used on the trip from home to work:

$$E = SOC_{max} - SOC \tag{26}$$

This is the minimum amount of energy the car will spend on its way back home. By dividing E with the electricity consumption (kWh/km) we obtain an approximation for the next free distance D.

References

[1] L. Fulton, P. Cazzola, F. Cuenot, K. Kojima, T. Onoda, J. Staub, and M. Taylor, *Transport, Energy and CO2: Moving toward Sustainability*. International Energy Agency, 2009.

[2] A. Burke and M. Miller, "Performance characteristics of lithium-ion batteries of various chemistries for plug-in hybrid vehicles," tech. rep., University of California-Davis, Institute of Transportation Studies, May 2009.

[3] S. C. Davis, S. W. Diegel, and R. G. Boundy, *Transportation Energy Data Book: Edition 30*. Oak Ridge National Laboratory, 2011.

[4] M. Fischer, M. Werber, and P. V. Schwartz, "Batteries: Higher energy density than gasoline?," *Energy Policy*, vol. 37, pp. 2639–2641, 2009.

[5] O. Sundström and C. Binding, "Planning electric-drive vehicle charging under constrained grid conditions," in *Power System Technology (POWERCON), 2010 International Conference on*, pp. 1–6, 2010.

[6] J. A. Peças Lopes, F. J. Soares, P. M. Almeida, and M. Moreira da Silva, "Smart charging strategies for electric vehicles: Enhancing grid performance and maximizing the use of variable renewable energy resources," in *EVS24 International Battery, Hybrid and Fuel Cell Electric Vehicle Symposium*, 2009.

[7] W. Kempton and J. Tomic, "Vehicle-to-grid power fundamentals: Calculating capacity and net revenue," *Journal of Power Sources*, vol. 144, pp. 268–279, 2005.

[8] W. Kempton and J. Tomic, "Vehicle-to-grid power implementation: From stabilizing the grid to supporting large-scale renewable energy," *Journal of Power Sources*, vol. 144, no. 1, pp. 280–294, 2005.

[9] W. Kempton, V. Udo, K. Huber, K. Komara, S. Letendre, S. Baker, D. Brunner, and N. Pearre, "A test of vehicle-to-grid (V2G) for energy storage and frequency regulation in the PJM system," tech. rep., University of Delaware, 2008.

[10] C. Guille and G. Gross, "The integration of PHEV aggregations into a power system with wind resources," in *Bulk Power System Dynamics and Control (iREP) - VIII (iREP), 2010 iREP Symposium*, pp. 1–9, August 2010.

[11] M. D. Galus, R. La Fauci, and G. Andersson, "Investigating PHEV wind balancing capabilities using heuristics and model predictive control," in *Power and Energy Society General Meeting, 2010 IEEE*, pp. 1–8, July 2010.

[12] The New York Times, "In a blackout, Nissan, Mitsubishi and Toyota E.V.'s could function as generators." `http://wheels.blogs.nytimes.com/2011/09/01`, September 2011.

[13] Nissan Motor Company Ltd, "Nissan unveils new power supply system through Nissan LEAF." http://www.nissan-global.com/EN/NEWS/2011/_STORY/110802-01-e.html, August 2011.

[14] W. Su and M.-Y. Chow, "Performance evaluation of a PHEV parking station using particle swarm optimization," in *Power and Energy Society General Meeting, 2011 IEEE*, 2011.

[15] W. Su and M.-Y. Chow, "Investigating a large-scale PHEV/PEV parking deck in a smart grid environment," in *North American Power Symposium (NAPS), 2011*, 2011.

[16] S. Bashash, S. J. Moura, J. C. Forman, and H. K. Fathy, "Plug-in hybrid electric vehicle charge pattern optimization for energy cost and battery longevity," *Journal of Power Sources*, vol. 196, no. 1, pp. 541–549, 2011.

[17] K. Mets, T. Verschueren, W. Haerick, C. Develder, and F. De Turck, "Optimizing smart energy control strategies for plug-in hybrid electric vehicle charging," in *Network Operations and Management Symposium Workshops (NOMS Wksps), 2010 IEEE/IFIP*, pp. 293–299, 2010.

[18] K. Clement, E. Haesen, and J. Driesen, "Coordinated charging of multiple plug-in hybrid electric vehicles in residential distribution grids," in *Power Systems Conference and Exposition, 2009. PSCE '09. IEEE/PES*, pp. 1–7, 2009.

[19] M. D. Galus, R. A. Waraich, and G. Andersson, "Predictive, distributed, hierarchical control of PHEVs in the distribution system of a large urban area incorporating a multi agent transportation simulation," in *Proceedings of the 17th Power Systems Computations Conference (PSCC)*, (Stockholm, Sweden), 2011.

[20] L. Gan, U. Topcu, and S. Low, "Optimal decentralized protocols for electric vehicle charging." http://resolver.caltech.edu/CaltechCDSTR:2011.009, 2010.

[21] C. Zhou, K. Qian, M. Allan, and W. Zhou, "Modeling of the cost of EV battery wear due to V2G application in power systems," *IEEE Transactions on Energy Conversion*, vol. 26, pp. 1041–1050, December 2011.

[22] H. Huo, Q. Zhang, M. Q. Wang, D. G. Streets, and K. He, "Environmental implication of electric vehicles in China," *Environmental Science & Technology*, vol. 44, pp. 4856–4861, 2010.

[23] M. Matsumoto and T. Nishimura, "Mersenne Twister: A 623-dimensionally equidistribute uniform pseudorandom number generator," *ACM Transactions on Modeling and Computer Simulation*, vol. 8, pp. 3–30, January 1998.

[24] City of Helsinki Urban Facts, "Helsinki by district 2008." www.hel.fi/tietokeskus, 2008.

[25] Helsinki: Finnish Transport Agency, "Official statistics of Finland: Finnish road statistics 2010." http://www.stat.fi/til/tiet/index_en.html, 2011.